Mathematical Biosciences 389 (2025) 109524

Contents lists available at ScienceDirect

Mathematical Biosciences

journal homepage: www.elsevier.com/locate/mbs

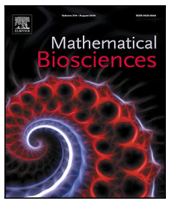

Dynamics of a pine wilt disease control model with nonlocal competition and memory diffusion

Yuting Ding [a], Pei Yu [b,*]

[a] College of Science, Northeast Forestry University, Harbin, Heilongjiang, 150040, PR China
[b] Department of Mathematics, Western University, London, Ontario, N6A 5B7, Canada

ARTICLE INFO

Keywords:
Pine wilt disease
Delayed reaction–diffusion equation
Memory diffusion
Nonlocal competition
Hopf bifurcation
Inhomogeneous periodic solutions

ABSTRACT

Pine wilt disease (PWD) is mainly spread by Monochamus alternatus (in short, M. alternatus). Woodpecker, as the natural predator of M. alternatus, is considered for biological prevention and controlling the PWD. In this paper, we propose a new M. alternatus-woodpecker model with nonlocal competition and memory-based diffusion, which makes the model more realistic for the PWD control. We focus on the dynamics and bifurcations of the model with various combinations of the memory diffusion and nonlocal competition. It is shown that the nonlocal competition can only cause the stable constant steady state to lose stability, while the memory-based diffusion can induce unstable spatially inhomogeneous periodic solutions due to Hopf bifurcation. Consequently, we can explain the spatiotemporal heterogeneity problem in ecology by innovatively using mathematical modelling. Normal form theory with the multiple time scales method is applied to particularly consider Hopf bifurcation, showing complex dynamical behaviours involving various oscillating motions. Finally, numerical simulations are presented with the parameter values chosen from the real forest data of Yuan'an County, Hubei Province, China, confirming the theoretical results of the spatiotemporal heterogeneity of forest diseases and pests, as well as the PWD control.

1. Introduction

Forest plays an irreplaceable role in regulating global carbon balance in the terrestrial ecosystem. However, forest pest and diseases seriously influence the forest carbon sink, and even damage global ecological environment to achieve the "carbon neutrality" goal [1]. Pine wilt disease (PWD) is caused by the pine wood nematode (also called Bursaphelenchus xylophilus), which is a devastating epidemic of pine trees. Once pine trees are infected, they will quickly die within 40 days, and the entire pine forest can be destroyed in about 3–5 years. The PWD spreads widely and rapidly and is difficult to be controlled, which has been well known as the "cancer" of pine tree species by forestry researchers [2,3].

The PWD was originated in North America, and more than 40 countries or regions in the world have listed pine wood nematodes as quarantine objects, for example, the introduced area of pines in Australia, Chili and South Africa; the pine cultivation area in New Zealand; the area without natural distribution of pines between latitude 25°N and 35°N; the prevailed area in Japan, China and Korea; the local area of several countries like in the USA and Mexico; in Portugal with Mediterranean climate, and so on [4].

The PWD discovered in China the first time was in 1982. Since then it has spread in 17 provinces in Mainland China, especially in coastal provinces such as Shandong, Zhejiang and Guangdong Provinces, with a total area of about 77 000 hectares, and it has caused huge ecological and economic losses for China [5,6]. The PWD is transmitted by the vector insect longhorn beetle which belongs to Monochamus (such as M. alternatus, M. sutor, M. galloprovincialis, M. carolinensis and so on, where M. is the abbreviation of Monochamus).

The transmission mechanism of the PWD is shown in Fig. 1. Each adult of the M. alternatus can carry thousands of nematodes. When the infected M. alternatus feed or lay eggs, and leave gnawing scars on healthy trees, pine wood nematodes escape from the trachea of M. alternatus and enter into the healthy pine trees. When the susceptible M. alternatus stay on the infected pine trees, they may be infected by the PWD, and then the PWD is spread further.

Many researchers established PWD models with a saturation incidence rate, and demonstrated how to reduce the number of infected populations by using pesticides periodicity [7,8]. Some optimal control strategies for controlling the PWD have been proposed [9,10]. Rahman et al. [11] discussed a host vector model of the PWD with a convex incident rate, while Wang et al. [12] explored the spatial distribution of M. alternatus based on the influence of meteorological factors.

* Corresponding author.
E-mail addresses: yuting840810@163.com (Y. Ding), pyu@uwo.ca (P. Yu).

https://doi.org/10.1016/j.mbs.2025.109524

Available online 8 September 2025

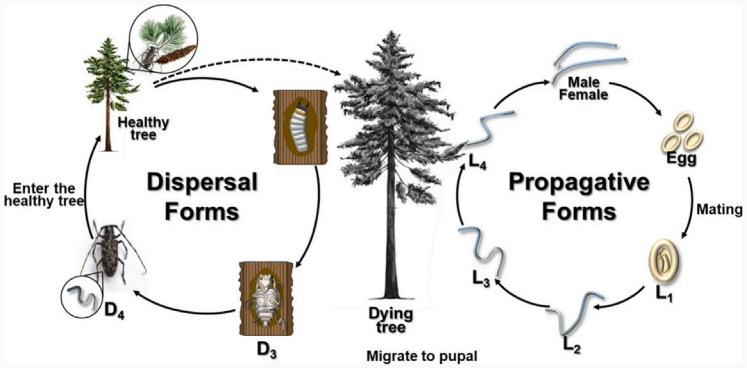

Fig. 1. The transmission mechanism of the pine wilt disease.

Recent studies have shown that spatial population movement plays an important role in resource consumption in certain locations. In reality, M. alternatus and its natural enemy spread freely in nature, and it has been found that the resource competition of M. alternatus located at a particular spatial point heavily depends on the densities in other spatial locations. Thus, it is necessary to develop a population model using reaction–diffusion equations in order to effectively control the PWD. Therefore, many scholars pay more attention to the complex dynamical properties of reaction–diffusion equations with nonlocal effect [13–19]. Although most of the systems introduce the kernel function of the nonlocal effect by using the average value of a spatial domain, it may also induce complex dynamics like spatially inhomogeneous periodic solutions. Recently, spatial memory and cognition of animals have drawn much attention in the mathematical modelling of animal movements. Many biologists observed through experiments that spatial memory has a significant impact on animal movement, and its cognitive process plays an important role in animal movement decision-making [20]. As a matter of fact, the woodpecker, as the predator of M. alternatus, has spatial memory and cognition, and it is thus more realistic to include the memory diffusion of woodpecker in the model for better controlling the PWD. The complex dynamics in the systems with memory diffusion has been studied by many researchers, for example, see [21–24]. The combination of memory-based diffusion and local effect may induce various complicated bifurcations such as Hopf bifurcation, double Hopf bifurcation, Turing–Hopf bifurcation, etc. which yield the spatial homogeneous/nonhomogeneous periodic solutions, the spatial homogeneous/nonhomogeneous steady states, and so on [25–27].

This paper is mainly motivated by the following facts.

(a) Study the biological prevention and control of the PWD. The key to control pine wood nematode is controlling the spread of the vector insect M. alternatus. There exist three main control methods: Biological control, chemical control and physical control. The biological pest control technology is one of the most safe and effective methods, and it usually achieves the control purpose by introducing the predacity enemy (such as woodpecker) or parasitical enemy (such as Dastarcus helophoroides and Scleroderma guani) of M. alternatus. In this paper, we establish a biological PWD control model by releasing the woodpecker as the predator of M. alternatus.

(b) Consider the spatiotemporal dynamics of a model with nonlocal competition and memory-based diffusion. To the best of our knowledge, there is only a few works using reaction–diffusion equations with both memory-based diffusion and nonlocal competition [25–27]. In this paper, we consider the nonlocal competition of M. alternatus and the averaged memory period of woodpecker, and propose a reaction–diffusion model with both memory diffusion and nonlocal effect. We will compare the dynamic properties of our system with and without nonlocal competition and memory diffusion to reveal why including memory diffusion and nonlocal competition makes the model more realistic.

The rest of the paper is organized as follows. In Section 2, we establish an M. alternatus-woodpecker model with nonlocal competition and memory-based diffusion associated with the PWD control. In Section 3, we analyse the dynamics of the established model with and without memory diffusion and nonlocal competition to show the importance of these two involvements. In Section 4, we derive the normal form of Hopf bifurcation and analyse the stability of the bifurcating periodic solutions. In Section 5, we first estimate the system parameter values based on real forest data, and then carry out numerical simulations to support the theoretical results. Finally, the conclusions and discussions are given in Section 6.

2. Mathematical modelling

In order to achieve the purpose for controlling the transmission of the PWD, forestry researchers usually release woodpeckers as the predator of M. alternatus according to biological control method.

2.1. ODE model

We first propose the following M. alternatus-woodpecker ordinary differential equation (ODE) model with Holling type-II functional response function associated with the PWD control,

$$\begin{cases} \dfrac{du(t)}{dt} = ru(t)\left(1-\dfrac{u(t)}{N}\right) - \dfrac{mu(t)v(t)}{1+u(t)} - b_1u(t) - ku(t), \\ \dfrac{dv(t)}{dt} = \dfrac{cmu(t)v(t)}{1+u(t)} - b_2v(t) + \Lambda, \end{cases} \tag{1}$$

where $u(t)$ and $v(t)$ represent the populations of M. alternatus and woodpecker at time t, respectively; r is the natural growth rate of M. alternatus; N is the capacity of environmental for M. alternatus; k is the mortality of M. alternatus caused by parasitical enemy and pathogenic microorganism; b_1 and b_2 denote the mortalities of M. alternatus caused by chemical and physical controls and by the woodpecker, respectively; m is the encounter rate of M. alternatus and woodpecker; c is the conversion rate of the generalist woodpecker; Λ is the input rate of woodpecker for biological control. All these parameters are positive real constants. Especially, we choose Holling type-II functional response function since M. alternatus is invertebrate.

For the nonnegativity and boundedness of the solutions of system (1), we have the following result.

Theorem 2.1. *Considering system (1) with initial conditions satisfying $u(0) = u_0 \geq 0$ and $v(0) = v_0 \geq 0$, then all the solutions of the system remain nonnegative and uniformly bounded.*

Proof. Firstly, we prove the nonnegativity by using a contradiction argument. Suppose that $u(t)$ is not always nonnegative for $t \geq 0$, namely there exists the first $t_1 > 0$ such that $u(t_1) = 0$ and $u'(t_1) < 0$. According to the first equation in system (1), we obtain $u'(t_1) = 0$, leading to a contradiction. Therefore, $u(t) \geq 0$ ($t \geq 0$). Similarly, assume that $v(t)$ is not always nonnegative for $t \geq 0$, namely there exists the first $t_2 > 0$ such that $v(t_2) = 0$ and $v'(t_2) < 0$. Based on the second equation in system (1), we obtain $v'(t_2) > 0$ due to $\Lambda > 0$, again giving rise to a contradiction, and so $v(t) \geq 0$ for $t \geq 0$. Thus, all the solutions of system (1) are nonnegative provided that the initial conditions are nonnegative.

Next, we show that the solution $u(t)$ of system (1) is uniformly bounded. From the first equation in system (1), we have

$$\frac{du(t)}{dt} \leq ru(t)\Big(1 - \frac{u(t)}{N}\Big), \quad \text{with} \quad u(0) = u_0,$$

for $t \geq 0$. Consider the equation,

$$\frac{dQ(t)}{dt} = rQ(t)\Big(1 - \frac{Q(t)}{N}\Big), \quad \text{with} \quad Q(0) = q_0.$$

It is easy to see that $\lim_{t\to+\infty} Q(t) = N$ for $q_0 > 0$. Thus, for any $\epsilon > 0$, there exists $T_0 > 0$ such that $Q(t) \leq N + \epsilon$ for $t \geq T_0$. By the standard comparison theorem of ODEs, we know that $u(t) \leq Q(t)$ is true for $t \geq 0$. Further, if we denote $Q_0 = \max_{0\leq t\leq T_0} Q(t)$, then it follows that $u(t) \leq Q(t) \leq \max\{Q_0, N + \epsilon\}$ for $t \geq 0$.

Let $w = cu + v$. Then, we have

$$\begin{aligned}\frac{\mathrm{d}w}{\mathrm{d}t} + b_2 w =& cru\Big(1 - \frac{u}{N}\Big) - b_1 cu - kcu + b_2 cu + \Lambda \leq c(r + b_2)u + \Lambda \\ \leq& c(c + b_2)\max\{Q_0, N + \epsilon\} + \Lambda.\end{aligned}$$

According to differential inequality, we obtain

$$\lim_{t\to+\infty} \sup w(t) \leq \frac{c(r + b_2)\max\{Q_0, N + \epsilon\} + \Lambda}{b_2}.$$

This completes the proof. □

Remark 1. The input rate Λ plays the main role in order to achieve the biological control by releasing woodpecker. Obviously, due to $\Lambda > 0$, the upper bound of the population of woodpecker $v(t)$ depends on Λ.

2.2. PDE model

Since the resource competition of M. alternatus depends on the densities of the whole spatial states, and woodpeckers have memory of the distribution of prey density at a past time, it is necessary to establish a reaction–diffusion equation for the PWD control. More detailed reasons for motivating us to develop such a model are described as follows.

(a) Introducing biological control: There are three main causes for the natural death of M. alternatus: (i) killed by the natural enemy, including predacity enemy and parasitical enemy; (ii) killed by pathogenic microorganism infection, such as fungi infection, bacteria infection and virus infection; and (iii) died due to deinsectization, such as biological control, chemical control and physical control. Biological pest control technology is one of the most safe and effective measures to decrease the amount of vector insect, M. alternatus, which is thus adopted as the main strategy for controlling the pine wood nematode. Thus, the system that we want to establish will mainly consider the effect of biological prevention and the PWD control, but also involves the influence of the chemical control and physical control, as well as the pathogenic microorganism infection. Moreover, the woodpecker, which is the predacity enemy of M. alternatus, is introduced into the system in terms of a constant input rate, and the aim of biological control is realized by releasing the woodpecker quantitatively.

(b) Introducing nonlocal competition of M. alternatus: Resource competition of M. alternatus located at a particular spatial point x heavily depends on the densities in other spatial locations. To describe this, we assume that the resource competition of M. alternatus depends on the weighted average of nearby populations in spatial location, by introducing the nonlocal competition in the form of $ru(x,t)\big(1 - \frac{\int_0^\pi G(x,y)u(y,t)\mathrm{d}y}{N}\big)$, in which $G(x,y) = \frac{1}{\pi}$ is a kernel function. Here, the meaning of this formula will be described below in Eq. (2).

(c) Introducing memory-based and cognition of the woodpecker: Woodpeckers have spatial memory and cognition, and they move towards the high density of M. alternatus at past averaged memory period. Thus, the memory-based diffusion term $\eta\mathrm{div}(v\nabla u) = \eta(v(x,t)u(x,t-\tau)_x)_x$ is introduced into the model. Again, the meaning of this formula will be given below.

To achieve the above goals, we introduce the Fickian diffusion to the ODE model (1) to obtain the following M. alternatus-woodpecker reaction–diffusion equation with Neumann boundary conditions. Moreover, it is assumed that the model has Holling type-II functional response with nonlocal effect and memory-based diffusion associated with the biological pest control of the PWD. Thus, we obtain the model described by PDE equations in the form of

$$\begin{cases} \dfrac{\partial u(x,t)}{\partial t} = d_1\Delta u(x,t) + ru(x,t)\Big(1 - \dfrac{\hat{u}(x,t)}{N}\Big) \\ \qquad\qquad - \dfrac{mu(x,t)v(x,t)}{1+u(x,t)} - (b_1 - k)u(x,t), \\ \dfrac{\partial v(x,t)}{\partial t} = d_2\Delta v(x,t) - \eta(v(x,t)u_x(x,t-\tau))_x + \dfrac{cmu(x,t)v(x,t)}{1+u(x,t)} \\ \qquad\qquad - b_2 v(x,t) + \Lambda, \\ \dfrac{\partial u(x,t)}{\partial \nu} = \dfrac{\partial v(x,t)}{\partial \nu} = 0, x \in \partial\Omega, t \geq 0, \\ u(x,\theta) = \varphi_u(x,\theta) \geq 0, v(x,\theta) = \varphi_v(x,\theta) \geq 0, x \in \Omega, \theta \in [-\tau, 0], \end{cases} \tag{2}$$

where $x \in \Omega, t \geq 0$, and $u(x,t)$ and $v(x,t)$ represent the population density of M. alternatus and woodpecker at time t and position x, respectively. $x \in \Omega = (0,\pi)$ is an open area with smooth boundary on $\mathbb{R}^{\mathrm{N}}$ ($\mathrm{N} \geq 1$). Among them, $\hat{u} = \int_0^\pi G(x,y)u(y,t)\mathrm{d}y$, where $G(x,y) = \frac{1}{\pi}$ is a kernel function on a one-dimensional spatial region Ω, ν is the outer normal vector of the boundary $\partial\Omega$, and Δ denotes the Laplace operator in $\mathbb{R}^{\mathrm{N}}$ ($\mathrm{N} \geq 1$). b_1 and k represent the influence of the chemical control and physical control, and the pathogenic microorganism infection, respectively. d_1 and d_2 are the spread rates of M. alternatus and woodpecker, respectively; η is the coefficient of memory-based diffusion, and $\eta \geq 0$ means that woodpeckers move towards the high density of M. alternatus; and τ is the averaged memory period. The definitions of other parameters are the same as those appearing in system (1), and all the parameters take positive real values.

3. Analysis for system (2)

3.1. Existence of positive constant steady state

System (2) has one boundary constant steady state $E_0 = (u_0, v_0) = (0, \frac{\Lambda}{b_2})$. Considering the biological meaning of the system (2), we are more interested in the existence of the positive constant steady state (PCSS). Let the PCSS be denoted by (u_1^*, v_1^*). To find them, simplify setting $\frac{\partial u}{\partial t} = \frac{\partial v}{\partial t} = d_1 = d_2 = \eta = 0$ in (2) we obtain

$$v_1^* = \frac{\Lambda(1 + u_1^*)}{b_2 + (b_2 - cm)u_1^*}, \tag{3}$$

and u_1^* is determined from the quadratic polynomial equation,

$$a_2(u_1^*)^2 + a_1 u_1^* + a_0 = 0, \tag{4}$$

where

$$a_2 = \frac{r}{N}(b_2 - cm),$$
$$a_1 = \frac{rb_2}{N} + (b_2 - cm)(b_1 + k - r), \tag{5}$$
$$a_0 = m\Lambda + b_2(b_1 + k - r).$$

Then, we have the following lemma for the existence of the PCSS of the system (2).

Lemma 3.1. *The PCSS of the system (2) and their existence conditions are given as follows.*

(1) If $b_2 - cm < 0$, then the PCSS is given by $E_1^- = (u_1^*, v_1^*)$, where

$$u_1^* = u_1^- = \frac{N}{2r(cm - b_2)}\left\{\frac{rb_2}{N} + (r - b_1 - k)(cm - b_2) - \sqrt{\left[\frac{rb_2}{N} - (cm - b_2)(r - b_1 - k)\right]^2 + \frac{4rm\Lambda}{N}(cm - b_2)}\right\},$$
$$r > b_1 + k + \frac{m\Lambda}{b_2},$$
$$v_1^* = v_1^- = \frac{\Lambda(1 + u_1^-)}{b_2 - (cm - b_2)u_1^+}.$$

(2) If $b_2 - cm = 0$, then the PCSS is given by

$$E_1^c = (u_1^*, v_1^*) = \left(\frac{N}{r}\left[r - \left(b_1 + k + \frac{m\Lambda}{b_2}\right)\right], \frac{\Lambda}{b_2}(1 + u_1^*)\right), \quad r > b_1 + k + \frac{m\Lambda}{b_2}.$$

(3) If $b_2 - cm > 0$, then the following results hold.

(a) When $a_0 < 0$, the system (2) has an unique PCSS:

$$E_1^{(1)} = (u_1^*, v_1^*) = \left(\frac{-a_1 + \sqrt{a_1^2 - 4a_0a_2}}{2a_2}, \frac{\Lambda(u_1^* + 1)}{b_2(u_1^* + 1) - cmu_1^*}\right).$$

(b) When $a_0 > 0$, $a_1^2 - 4a_0a_2 = 0$ and $a_1 < 0$, the system (2) has a unique PCSS:

$$E_1^{(2)} = (u_1^*, v_1^*) = \left(-\frac{a_1}{2a_2}, \frac{\Lambda(2a_2 - a_1)}{b_2(2a_2 - a_1) + cma_1}\right).$$

(c) When $a_0 > 0$, $a_1^2 - 4a_0a_2 > 0$ and $a_1 < 0$, the system (2) has two PCSS:

$$E_{1,2} = (u_{1,2}^*, v_{1,2}^*) = \left(\frac{-a_1 \pm \sqrt{a_1^2 - 4a_0a_2}}{2a_2}, \frac{\Lambda(u_{1,2}^* + 1)}{b_2(u_{1,2}^* + 1) - cmu_{1,2}^*}\right).$$

Proof. The proofs for the items (2) and (3) are straightforward, we only prove the item (1). First, note that $v_1^* > 0$ requires the condition:

$$b_2 + (b_2 - cm)u_1^* > 0 \quad \Longrightarrow \quad u_1^* < \frac{b_2}{cm - b_2}.$$

Then, the quadratic equation (4) becomes

$$\frac{r}{N}(cm - b_2)(u_1^*)^2 - \left[\frac{rb_2}{N} + (cm - b_2)(r - b_1 - k)\right]u_1^* + b_2\left(r - b_1 - k - \frac{m\Lambda}{b_2}\right) = 0,$$

which has the discriminant,

$$\Delta_1 = \left[\frac{rb_2}{N} - (cm - b_2)(r - b_1 - k)\right]^2 + \frac{4rm\Lambda}{N}(cm - b_2) > 0, \tag{6}$$

implying that the quadratic polynomial equation always has 2 real solutions and the bigger one is always positive. Let the two solutions be $u_1^{\pm}$. Then, it is easy to prove that $u_1^- < \frac{b_2}{cm - b_2} < u_1^+$ by a direct computation:

$$\begin{aligned} & u_1^- < \frac{b_2}{cm - b_2} < u_1^+ \\ \Longleftrightarrow \quad & \frac{N\left[\frac{rb_2}{N} + (r - b_1 - k)(cm - b_2) - \sqrt{\Delta_1}\right]}{2r(cm - b_2)} < \frac{b_2}{cm - b_2} < \frac{N\left[\frac{rb_2}{N} + (r - b_1 - k)(cm - b_2) + \sqrt{\Delta_1}\right]}{2r(cm - b_2)} \\ \Longleftrightarrow \quad & -\sqrt{\Delta_1} < \frac{rb_2}{N} - (r - b_1 - k)(cm - b_2) < \sqrt{\Delta_1}, \end{aligned}$$

which is obviously true. Then, the possible solution is $u_1^- > 0$, which requires the condition: $r > b_1 + k + \frac{m\Lambda}{b_2}$. □

Fig. 2 shows the existence of PCSS of the system (2). The yellow region in Fig. 2(1) denotes $r > b_1 + k + \frac{m\Lambda}{b_2}$ for $b_2 - cm < 0$, in which system (2) has a unique PCSS E_1^-, corresponding to the case (1) in Lemma 3.1. The yellow region in Fig. 2(2) denotes $r > b_1 + k + \frac{m\Lambda}{b_2}$ for $b_2 - cm = 0$, in which system (2) has a unique PCSS E_1^c, corresponding to the case (2) in Lemma 3.1. The yellow region in Fig. 2(3) denotes $a_0 < 0$, in which the system (2) has a unique PCSS $E_1^{(1)}$, corresponding to the case (3a) in Lemma 3.1. On the blue line, $a_1^2 - 4a_0a_2 = 0$ satisfying $a_0 > 0$ and $a_1 < 0$, the system (2) has a unique PCSS $E_1^{(2)}$, corresponding to the case (3b) in Lemma 3.1. The flesh pink region means $a_0 > 0$, $a_1^2 - 4a_0a_2 > 0$ and $a_1 < 0$, in which the system (2) has two PCSS $E_{1,2}$, corresponding to the case (3c) in Lemma 3.1. To have a clear viewing, we zoom a small region around the intersection point of the curves $a_1 = 0$, $a_0 = 0$ and $a_1^2 - 4a_0a_2 = 0$, to obtain the small figure depicted in Fig. 2(3).

It can be seen from Fig. 2 that if the input rate of woodpecker Λ is larger, then less mortality of M. alternatus b_1 induced by chemical control and physical control is needed, and the PCSS exists. Similarly, if the mortality of M. alternatus b_1 is larger, then smaller input rate Λ is needed for the system (2) to have PCSS. Actually, b_1 as the mortality of M. alternatus induced by chemical and physical control, and k as the mortality of M. alternatus induced by pathogenic microorganism infection, yield the same status of the system to exist for controlling pest. This implies that regardless which control method is used, the PCSS can always exist, which is consistent with the actual ecological situation. Moreover, if both Λ and b_1 are large, then the system (2) cannot have PCSS, which implies that excessive control for the PWD, no matter which method used, is not beneficial to the balance of ecosystem.

3.2. Bifurcation analysis for system (2)

In this section, we will analyse the dynamics of system (2) with and without memory diffusion and nonlocal competition, since we are interested in the impact of memory-based of Woodpecker and nonlocal competition of M. alternatus on controlling the PWD. Without loss of generality, we assume that one condition of the five cases in Lemma 3.1 is satisfied, and the system (2) has a PCSS, denoted by $E_* = (u^*, v^*)$.

3.2.1. System (2) without diffusion

Assume that the system (2) does not contain spatial diffusion, then it is obvious that the system also does not have memory diffusion nor nonlocal competition, resulting in the system (1). The characteristic equation at $E_* = (u^*, v^*)$ of system (1) is given by

$$\lambda^2 + A_0\lambda + F_0 = 0, \tag{7}$$

where

$$\begin{aligned} & A_0 = \frac{ru^*}{N} - a_{11} - a_{22}, \quad F_0 = a_{11}a_{22} - a_{12}a_{21} - \frac{ru^*a_{22}}{N}, \\ & a_{22} = \frac{cmu^*}{u^* + 1} - b_2, \\ & a_{11} = r - b_1 - k - \frac{ru^*}{N} - \frac{mv^*}{(1 + u^*)^2}, \quad a_{12} = -\frac{mu^*}{u^* + 1}, \\ & a_{21} = \frac{cmv^*}{(u^* + 1)^2}. \end{aligned} \tag{8}$$

It is obvious that $a_{12} < 0$, $a_{21} > 0$, and $a_{22} = \frac{u^*(cm - b_2) - b_2}{1 + u^*} < 0$ when $b_2 - cm \geq 0$. Next, we prove that $a_{22} < 0$ also holds when $b_2 - cm < 0$. Therefore, it is always true that $a_{22} < 0$ regardless the sign of $b_2 - cm$, and then the equilibrium E_* can include all the three cases listed in Lemma 3.1. When $b_2 - cm < 0$, $a_{22} < 0$ if $u^* < \frac{b_2}{cm - b_2}$. For the case $b_2 - cm < 0$, the solution is $u^* = u_1^-$. We show that $u_1^- < \frac{b_2}{cm - b_2}$, which is equivalent to (noticing that Δ_1 is given in (6))

$$\begin{aligned} & \frac{N}{2r(cm - b_2)}\left[\frac{rb_2}{N} + (r - b_1 - k)(cm - b_2) - \sqrt{\Delta_1}\right] < \frac{b_2}{cm - b_2}, \\ & \quad \text{subject to } r > b_1 + k + \frac{m\Lambda}{b_2} \\ \Longleftrightarrow \quad & (r - b_1 - k)(cm - b_2) - \frac{rb_2}{N} < \sqrt{\Delta_1}, \end{aligned}$$

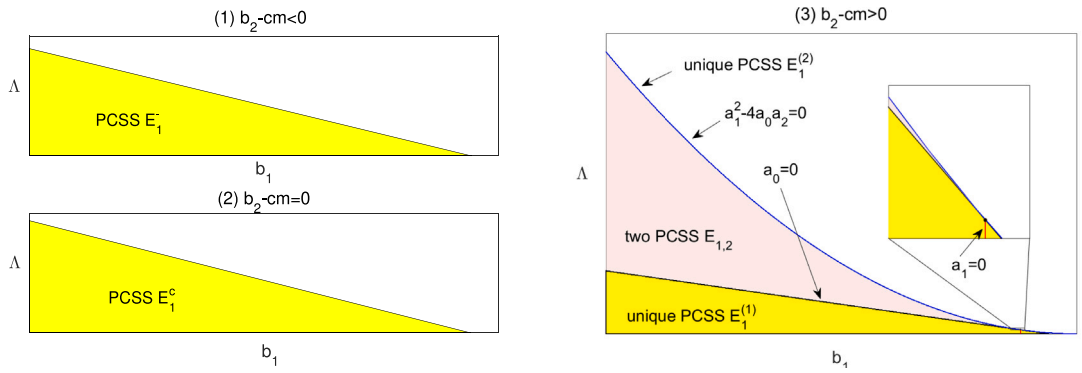

Fig. 2. Existence of the PCSS of system (2).

which holds for $N \le \frac{rb_2}{(r-b_1-k)(cm-b_2)}$. When $N > \frac{rb_2}{(r-b_1-k)(cm-b_2)}$, the above inequality is equivalent to

$$\left[(r-b_1-k)(cm-b_2)-\frac{rb_2}{N}\right]^2-\Delta_1<0 \iff -\frac{4rm\Lambda}{N}(cm-b_2)<0.$$

For convenience of discussing the stability of the equilibrium E_*, we make the following assumption:

$$(H_1)\quad A_0>0,\ F_0>0, \tag{9}$$

where A_0 and F_0 are given in (8). It is well known that all the roots of the characteristic equation (7) have negative real part when (H_1) holds, implying that E_* is locally asymptotically stable (LAS), while it is unstable if (H_1) does not hold.

We have the following theorem.

Theorem 3.2. *The following conclusions are true for the positive equilibrium E_* of the system (1) without spatial diffusion under which (1) becomes an ODE equation.*

(1) When $A_0>0$ and $F_0>0$ (i.e., (H_1) holds), E_* is LAS.
(2) When $A_0<0$ or $F_0<0$, E_* is unstable.
(3) When $F_0=0$, the system undergoes a fixed point bifurcation near E_*.
(4) When $A_0=0,\ F_0>0$, the system undergoes a Hopf bifurcation near E_*.

3.2.2. System (2) with diffusion

Next, we will consider four different cases in the system (2): Without nonlocal effect and memory diffusion; with nonlocal effect but without memory diffusion; with memory diffusion but without nonlocal competitive; and with both nonlocal effect and memory diffusion. Then, we will compare the dynamics for the four cases to reveal the effectiveness of the memory diffusion and nonlocal competitive on the system's dynamics. For convenience of a comparison, we consider the following unified characteristic equation of the system (2) evaluated at $E_* = (u^*, v^*)$ for all the four cases:

$$\lambda^2+\left(A_n-p_1\delta_n\frac{ru^*}{N}\right)\lambda+F_n+p_2\left(\delta_n a_{22}-d_2n^2\right)\frac{ru^*}{N}+p_3C_n\mathrm{e}^{-\lambda\tau}=0, \tag{10}$$

where $p_i=1$ or 0 $(i=1,2,3)$, $n\in \mathrm{N}=\{0,1,2,\dots\}$, and

$$A_n=d_1n^2+d_2n^2+A_0,$$
$$F_n=d_1d_2n^4+\left[d_2\left(\frac{ru^*}{N}-a_{11}\right)-a_{22}d_1\right]n^2+F_0,$$
$$C_n=-a_{12}n^2\eta v^*,$$

with A_0, F_0, a_{11}, a_{12}, a_{21} and a_{22} given in (8), and $\delta_n=0$ (or 1) if $n=0$ (or $n\neq 0$). Actually, when $p_i=0$ $(i=1,2,3)$ and $n=0$, Eq. (10) becomes (7).

When $\tau=0$, Eq. (10) can be rewritten as

$$\lambda^2+\left(A_n-p_1\delta_n\frac{ru^*}{N}\right)\lambda+F_n+p_2\left(\delta_n a_{22}-d_2n^2\right)\frac{ru^*}{N}+p_3C_n=0,$$

$$n\in \mathrm{N}=\{0,1,2,\dots\}. \tag{11}$$

For the convenience of discussing the stability of the equilibrium E_*, we make the following assumption:

$$(H_2)\quad d_1+d_2-a_{11}-a_{22}>0. \tag{12}$$

Note that if $p_1=0$ or $n=0$, then $A_n-p_1\delta_n\frac{ru^*}{N}=A_n\ge A_0>0$ when (H_1) holds; and if $p_1\neq 0$ and $n\neq 0$, then $A_n-p_1\delta_n\frac{ru^*}{N}=d_1n^2+d_2n^2-a_{11}-a_{22}>0$ when (H_2) holds. Further, let $y=n^2$ and denote that

$$\begin{aligned} l(y) &\triangleq F_n+p_2\left(\delta_n a_{22}-d_2y\right)\frac{ru^*}{N}+p_3C_n\\ &=d_1d_2\,y^2-My+F_0+p_2a_{22}\delta_n\frac{ru^*}{N},\\ M&=d_2a_{11}+d_1a_{22}+p_3a_{12}\eta v^*+(p_2-1)d_2\frac{ru^*}{N},\\ \delta&=M^2-4d_1d_2\left(F_0+p_2a_{22}\delta_n\frac{ru^*}{N}\right),\\ k_*&=\left[\sqrt{\frac{M}{2d_1d_2}}\right],\quad \text{for } M\ge 0, \end{aligned} \tag{13}$$

where the notation $[\cdot]$ for k_* denotes the largest integer that is not greater than the given real number. Then, we have following theorem.

Theorem 3.3. *When $\tau=0$, for the system (2) without nonlocal competition under the assumption (H_1), and for the system (2) with nonlocal competition under the assumptions (H_1) and (H_2), if one of following conditions hold:*

(1) $M\le 0$;
(2) $M>0$ and $\delta\le 0$;
(3) $M>0$, $\delta>0$, $l(k_*^2)>0$ and $l((k_*+1)^2)>0$,

then E_* is LAS. Otherwise, E_* is unstable.

Proof. If $A_n-p_1\delta_n\frac{ru^*}{N}>0$ and $l(n^2)=F_n+p_2\left(\delta_n a_{22}-d_2n^2\right)\frac{ru^*}{N}+p_3C_n>0$, then all the roots of Eq. (11) have negative real parts, implying that E_* is LAS.

Actually, when $\tau=0$, for the system (2) without nonlocal competition, i.e., $p_1=p_2=0$, we have $A_n-p_1\delta_n\frac{ru^*}{N}=A_n>A_0>0$ under the assumption (H_1); while for the system (2) with nonlocal competition, i.e., $p_1=p_2=1$, we obtain $A_n-p_1\delta_n\frac{ru^*}{N}=d_1n^2+d_2n^2-a_{11}-a_{22}>0$ if the assumption (H_2) holds. Thus, we only need to consider the function $l(y)$ for $y=n^2\ge 0$. Noticing that $l(0)=F_0>0$, and the graph of $l(y)$ opens upward, we have following conclusions.

(1) If $M\le 0$, it is obvious that $l(y)>0$ for $y\ge 0$, since all coefficients in the quadratic polynomial $l(y)$ are either positive or non-negative.
(2) If $M>0$ and $\delta\le 0$, then the quadratic polynomial $l(y)$ has two negative real roots, and thus $l(y)>0$ for $y\ge 0$.

(3) If $M > 0$ and $\delta > 0$, then the vertex of the function $l(y)$ is located on the positive y-axis. Therefore, the requirement that $l(y) > 0$ for all $y = n^2$ is guaranteed under the conditions $l(k_*^2) > 0$ and $l((k_* + 1)^2) > 0$.

Thus, if one of above two conditions holds, E_* is LAS. Otherwise, E_* is unstable. □

When $\tau > 0$, suppose that $\lambda = \mathrm{i}\omega$ ($\omega > 0$) is a root of the second characteristic equation in (10) with $p_3 = 1$ due to the delay. Then, we have that

$$\omega^2 - F_n - p_2\left(\delta_n a_{22} - d_2 n^2\right)\frac{ru^*}{N} = C_n \cos(\omega\tau),$$
$$\left(A_n - p_1\delta_n \frac{ru^*}{N}\right)\omega = C_n \sin(\omega\tau),$$

which yields the 2nd-degree polynomial equation:

$$h(z) \triangleq z^2 + P_n z + Q_n = 0, \tag{14}$$

where $n \in \mathrm{N}_+ = \{1, 2, \ldots\}$, $z = \omega^2$, and

$$\begin{cases} P_n = \left(A_n - p_1\delta_n \frac{ru^*}{N}\right)^2 - 2F_n - 2p_2\left(\delta_n a_{22} - d_2 n^2\right)\frac{ru^*}{N}, \\ Q_n = \left[F_n + p_2\left(\delta_n a_{22} - d_2 n^2\right)\frac{ru^*}{N}\right]^2 - C_n^2, \end{cases}$$

If $Q_n < 0$, Eq. (14) has a unique positive root, $z_1 = \frac{1}{2}\left(-P_n + \sqrt{\Delta_*}\right)$, where $\Delta_* = P_n^2 - 4Q_n$; while if $Q_n > 0$, we have $\Delta_* > 0$ and assume that $P_n < 0$, under which Eq. (14) has two positive roots, $z_{1,2} = \frac{1}{2}\left(-P_n \pm \sqrt{\Delta_*}\right)$.

Note that $\omega = \sqrt{z_k}$ ($k = 1, 2$) and $C_n > 0$. Therefore, for the system (2) without nonlocal competition under the assumption (H_1), and for the system (2) with nonlocal competition under the assumptions (H_1) and (H_2), $A_n - p_1\delta_n \frac{ru^*}{N} > 0$ obviously, thus, we obtain the critical delay τ, given by

$$\tau_{n,k}^{(j)} = \frac{1}{\omega_k}\left(2j\pi + \arccos\frac{\omega^2 - F_n - p_2\left(\delta_n a_{22} - d_2 n^2\right)\frac{ru^*}{N}}{C_n}\right), \tag{15}$$

where $k = 1, 2$; $j = 0, 1, 2, \ldots$; $n = 0, 1, 2, \ldots$.

Taking τ as a bifurcation parameter yields the following transversality condition to be held,

$$\mathrm{Re}\left(\frac{\mathrm{d}\lambda}{\mathrm{d}\tau}\Big|_{\tau=\tau_n^{(j)}}\right)^{-1} = \frac{h'(z_k)}{C_n^2} \neq 0, \tag{16}$$

then, we have the following result.

Theorem 3.4. *For the system (2) without nonlocal competition under the assumption (H_1), and for the system (2) with nonlocal competition under the assumptions (H_1) and (H_2), if one of the conditions in Theorem 3.3 is satisfied, then the PCSS E_* has the following properties.*

(1) If $P_n > 0$ and $Q_n > 0$, Eq. (14) has no positive roots, and E_* of the system is LAS for $\tau \geq 0$.

(2) Assume that $n_k \in I_1$, where $I_1 = \{n_{k_1}, n_{k_2}, \ldots, n_{k_m}\}$ or $\{n_{k_1}, n_{k_2}, \ldots, n_{k_m}, \ldots\} \subset \mathrm{N}_+$ (finite or infinite) satisfying $Q_n < 0$, and that $n_i \in I_2$, and $I_2 = \{n_{i_1}, n_{i_2}, \ldots, n_{i_l}\}$ or $\{n_{i_1}, n_{i_2}, \ldots, n_{i_l}, \ldots\} \subset \mathrm{N}_+$ (finite or infinite) satisfying $Q_n > 0$, $\Delta_* > 0$ and $P_n < 0$. Then, the following holds:

(a) if $I_1 \neq \emptyset$, $I_2 = \emptyset$, and suppose that the delay τ^* corresponding to n_{k^*} is the smallest critical delay, then E_* is LAS for $0 < \tau < \tau^*$ and unstable for $\tau > \tau^*$. Moreover, the system (2) undergoes Hopf bifurcation at $\tau = \tau_{n_k,1}^{(j)}$, $n_k \in I_1$,

(b) if $I_1 = \emptyset$, $I_2 \neq \emptyset$, and suppose that the delay τ^* corresponding to n_{i*} is the smallest critical delay, then E_* is LAS, and there may exist stability switches for $\tau > \tau^*$, where $\tau^* = \min\{\tau_{n_i,k}^{(0)}\}$, $n_i \in I_2, k = 1, 2$. Moreover, the system (2) undergoes Hopf bifurcation at $\tau = \tau_{n_i,k}^{(j)}$,

(c) if $I_1 \neq \emptyset$, $I_2 \neq \emptyset$, and suppose that the delay τ^* corresponding to n_* is the smallest critical delay, then E_* is LAS for $0 < \tau < \tau^*$, and there may exist stability switches for $\tau > \tau^*$, where $\tau^* = \min\{\tau_{n,k}^{(0)}\}$, $n \in I_1$ or I_2, $k = 1, 2$. Moreover, the system (2) undergoes Hopf bifurcation at $\tau = \tau_{n,k}^{(j)}$,

where $\tau_{n,k}^{(j)}$ is given in (15).

(3) If the parameters satisfy the condition in this theorem, and I_1 or I_2 is nonempty infinite set, but $\tau^* \to 0$ as $n \to \infty$, then E_* of the system is always unstable for $\tau \geq 0$.

(4) If there exists n_1 satisfying $Q(n_1) = 0$, then the system (2) undergoes n_1-mode Turing bifurcation. Especially, if there also exists some n_2 satisfying one of the conditions (a), (b) and (c) in the case (2), then the system (2) undergoes an n_1-n_2-mode Turing–Hopf bifurcation.

Proof. If E_* is LAS for system (2) with $\tau = 0$, then we have following results.

(1) It is obvious that Eq. (14) has no positive roots under the conditions $P_n > 0$ and $Q_n > 0$, indicating that the system (2) cannot have Hopf bifurcation near E_*, and thus E_* is LAS for $\tau \geq 0$.

(2) If there exists $n_k \in I_1$, and $I_1 = \{n_{k_1}, n_{k_2}, \ldots, n_{k_m}\}$ or $\{n_{k_1}, n_{k_2}, \ldots, n_{k_m}, \ldots\} \subset \mathrm{N}_+$ (finite or infinite) satisfying $Q_n < 0$, then Eq. (2) has one positive root for $n = n_k$ ($k = k_1, k_2, \ldots, k_m, \ldots$); while if there exists $n_i \in I_2$, and $I_2 = \{n_{i_1}, n_{i_2}, \ldots, n_{i_l}\}$ or $\{n_{i_1}, n_{i_2}, \ldots, n_{i_l}, \ldots\} \subset \mathrm{N}_+$ (finite or infinite) satisfying $Q_n > 0$, $\Delta_* > 0$ and $P_n < 0$, then Eq. (2) has two positive roots for $n = n_i$ ($i = i_1, i_2, \ldots, i_l, \ldots$). There are three subcases.

(a) If $I_1 \neq \emptyset$, $I_2 = \emptyset$, and suppose that τ^* corresponding to n_{k^*} is the smallest critical delay, then E_* is LAS for $0 < \tau < \tau^*$ and unstable for $\tau > \tau^*$. Moreover, the system (2) undergoes Hopf bifurcation at $\tau = \tau_{n_k,1}^{(j)}$, $n_k \in I_1$, where $\tau_{n_k,1}^{(j)}$ is given in (15).

(b) If $I_1 = \emptyset$, $I_2 \neq \emptyset$, and suppose that τ^* corresponding to n_{i*} is the smallest critical delay, then E_* is LAS, and there may exist stability switches between $\tau_{n_k,1}^{(j)}$ for $\tau > \tau^*$, where $\tau^* = \min\{\tau_{n_i,k}^{(0)}\}$, $n_i \in I_2$, $k = 1, 2$. Moreover, the system (2) undergoes Hopf bifurcation at $\tau = \tau_{n_i,k}^{(j)}$, where $\tau_{n_i,k}^{(j)}$ is given in (15).

(c) If $I_1 \neq \emptyset$, $I_2 \neq \emptyset$, and suppose that τ^* corresponding to n_* is the smallest critical delay, then E_* is LAS for $0 < \tau < \tau^*$, and there may exist stability switches between $\tau_{n_i,k}^{(j)}$ for $\tau > \tau^*$, where $\tau^* = \min\{\tau_{n,k}^{(0)}\}$, $n \in I_1$ or I_2, $k = 1, 2$. Moreover, the system (2) undergoes Hopf bifurcation at $\tau = \tau_{n,k}^{(j)}$, where $\tau_{n,k}^{(j)}$ is given in (15).

(3) When I_1 or I_2 is a nonempty infinite set, but $\tau^* \to 0$ as $n \to \infty$, there does not exist a minimum stable interval for τ, and thus E_* is always unstable for $\tau \geq 0$.

(4) When there exists an $n = n_1$ satisfying $Q(n_1) = 0$, Eq. (10) has one zero root, yielding an n_1-mode Turing bifurcation. In addition, if there exists another $n = n_2$ satisfying one of the conditions (a), (b) and (c) in the case (2), then the system (2) undergoes an n_1-n_2-mode Turing–Hopf bifurcation. □

Next, based on the above general results, we will compare the dynamics for the system with or without nonlocal competition and memory diffusion in the following four cases.

Case 1: The system (2) without nonlocal competition and memory diffusion, for which the characteristic equation of the system (2) evaluated at $E_* = (u^*, v^*)$ is given by Eq. (10) with $p_1 = p_2 = p_3 = 0$, that is,

$$\lambda^2 + A_n\lambda + F_n = 0, \quad n \in \mathrm{N}_+ = \{0, 1, 2, \ldots\}. \tag{17}$$

Comparing Eqs. (7) and (17), we note that the constant steady state E_* of system (1) without spatial diffusion ($d_1 = d_2 = 0$ or $n = 0$) is LAS when (H_1) holds, while E_* of system (2) without nonlocal competition and memory diffusion (but $d_1 d_2 \neq 0$) can be LAS, only if (H_1) holds, together with one of the conditions in Theorem 3.3 to be satisfied for $p_1 = p_2 = p_3 = 0$. This means that the conditions for stability of the PCSS are stronger when the self-diffusion is introduced, indicating that in nature the introduction of the spatial factors makes the control of the PWD more complicated.

Case 2: The system (2) with nonlocal effect but without memory diffusion, for which the characteristic equation of the system (2) evaluated at $E_* = (u^*, v^*)$ is given by Eq. (10) with $p_1 = p_2 = 1$ and $p_3 = 0$, that is,

$$\begin{aligned}&\lambda^2 + A_0\lambda + F_0 = 0, \quad n = 0,\\ &\lambda^2 + \left(A_n - \frac{ru^*}{N}\right)\lambda + F_n + \left(a_{22} - d_2 n^2\right)\frac{ru^*}{N} = 0, \quad n \in \mathrm{N}_+ = \{1, 2, \ldots\}.\end{aligned} \tag{18}$$

We compare (18) with (17), that is, compare the cases with and without nonlocal competition (but both without the memory diffusion). Note that $F_n = (d_1 n^2 + \frac{ru^*}{N} - a_{11})(d_2 n^2 - a_{22}) - a_{12}a_{21}$. Thus, when $d_2 - a_{22} > 0$, if the constant steady state of the system with nonlocal competition is LAS, then it must be also LAS for the system without nonlocal competition. This implies that when the spread rate of woodpecker, d_2, is large, the nonlocal competition within the species of M. alternatus is beneficial for their growth, but it has negative impact on the control of the PWD and the balance of the ecosystem.

Case 3: The system (2) with memory diffusion and without nonlocal competition, for which the characteristic equation of the system (2) evaluated at $E_* = (u^*, v^*)$ is given by Eq. (10) with $p_1 = p_2 = 0$, and $p_3 = 1$, that is,

$$\lambda^2 + A_n\lambda + F_n + C_n e^{-\lambda\tau} = 0, \quad n \in \mathrm{N}_+ = \{0, 1, 2, \ldots\}. \tag{19}$$

Without considering the nonlocal competition, we compare the system with and without the memory diffusion, that is, compare the systems (19) and (17). It is seen from the characteristic equation (19) for the system with memory diffusion but without nonlocal competition that it has one more positive term $C_n e^{-\lambda\tau}$ than the characteristic equation (17) for the system without memory diffusion and nonlocal competition due to $C_n > 0$. It should be pointed out that if the constant steady state of the system (2) without nonlocal competition and memory diffusion is LAS, then that of the system without memory diffusion and nonlocal competition with $\tau = 0$ must be LAS. However, it may not always be LAS for $\tau > 0$, since the transcendental function involved in the characteristic equation can cause more complicated bifurcation phenomenon such as periodic fluctuations to occur when the memory diffusion of woodpecker is introduced, which is consistent with the actual ecological situation. In fact, in this situation, woodpecker will peck M. alternatus effectively during its memory period, and its pecking ability will decrease near its critical memory period, which may cause the population density to fluctuate periodically.

Case 4: The system (2) with both nonlocal competition and memory diffusion, for which the characteristic equation of the system (2) evaluated at $E_* = (u^*, v^*)$ is given by Eq. (10) with $p_1 = p_2 = p_3 = 1$, that is,

$$\begin{aligned}&\lambda^2 + A_0\lambda + F_0 = 0, \quad n = 0,\\ &\lambda^2 + \left(A_n - \frac{ru^*}{N}\right)\lambda + F_n + \left(a_{22} - d_2 n^2\right)\frac{ru^*}{N} + C_n e^{-\lambda\tau} = 0,\\ &n \in \mathrm{N}_+ = \{1, 2, \ldots\}.\end{aligned} \tag{20}$$

Note that the second equation in (20) for the system with both memory diffusion and nonlocal competition has one more positive term $C_n e^{-\lambda\tau}$ than the characteristic equation (18) for the system without memory diffusion and with nonlocal competition, thus making it easy to generate bifurcations near the constant steady states of the system (2) with the memory diffusion when the nonlocal competition of M. alternatus is introduced. Similar to the explanation given for Case 3, we conclude that if the memory period of woodpecker is less than the critical delay, then woodpecker will peck M. alternatus more easily, and if the memory period is larger than (but still in the neighbourhood of) the critical delay, then the population density of M. alternatus and woodpecker will fluctuate periodically. This shows that stability of the spatial periodic solutions with nonlocal competition may be different from the system without nonlocal competition, implying that the nonlocal competition of M. alternatus may make M. alternatus easy to get more food from the competing resources in different spatial locations, so that avoid to be tracked by woodpecker. This observation will be confirmed by the simulation results (see Table 3 in Section 5).

To end this section, we want to emphasize a key important fact presented in Theorems 3.2–3.4: The results show that the nonlocal competition of M. alternatus has greater influence on the stability of the constant steady state, and the memory diffusion makes it easy to induce bifurcation of periodic solutions.

4. Hopf bifurcation analysis using normal form

In this section, we will derive the normal form of Hopf bifurcation for system (2) by using the multiple time scales (MTS) method. We focus on the averaged memory period of woodpecker τ, and study the impact of the delay on the change of population density. When $\tau = \tau_c = \tau_{n,k}^{(j)}$, where $\tau_{n,k}^{(j)}$ is given in (15), the characteristic equation (10) has eigenvalue $\lambda = \mathrm{i}\omega$ for $n = n_0 > 0$ at which the system (2) undergoes an n_0−mode Hopf bifurcation from the equilibrium $E_* = (u_*, v_*)$. Let $\tau = \tau_c + \varepsilon\mu$, where μ is the disturbance parameter, and ε is the dimensionless scale parameter.

Transferring the constant steady state $E_* = (u^*, v^*)$ of system (2) to the origin and rescaling time by $t \to \frac{t}{\tau}$, we obtain the Taylor expansion of the system (2) truncated at the cubic order terms, give by

$$\begin{cases}\dfrac{\partial u}{\partial t} = \tau\Big[d_1\Delta u + a_{11}u + a_{12}v - \dfrac{r(u^*+u)\hat{u}}{N} + \dfrac{m(v^*+v)u^2}{(u^*+1)^3}\\ \qquad\qquad - \dfrac{muv}{(u^*+1)^2} - \dfrac{mv^*u^3}{(u^*+1)^4}\Big],\\ \dfrac{\partial v}{\partial t} = \tau\left[d_2\Delta v + a_{21}u + a_{22}v - \eta v_x u_x(t-1) - \eta(v^*+v)u_{xx}(t-1)\right]\\ \qquad\qquad + \tau mc\,u\Big[\dfrac{v}{(u^*+1)^2} - \dfrac{(v^*+v)u}{(u^*+1)^3} + \dfrac{v^*u^2}{(u^*+1)^4}\Big],\\ \dfrac{\partial u(x,t)}{\partial \nu} = \dfrac{\partial v(x,t)}{\partial \nu} = 0, \ x \in \partial\Omega, \ t \geq 0,\\ u(x,t) = \varphi_u(x,t) \geq 0, \ v(x,t) = \varphi_v(x,t) \geq 0, \ x \in \Omega, \ t \in [-1, 0],\end{cases} \tag{21}$$

where a_{11}, a_{12}, a_{21} and a_{22} are given in (8).

Let $h = \left(1, h_1\right)^{\mathrm{T}}$ be the eigenvector of the linear operator of Eq. (21) at E_* corresponding to the eigenvalue $\mathrm{i}\,\omega\tau$, and $h^* = l\left(h_1^*, 1\right)^{\mathrm{T}}$ be the normalized eigenvector of the adjoint operator of the linear operator corresponding to the eigenvalue $-\mathrm{i}\,\omega\tau$, satisfying the inner product,

$$\langle h^*, h\rangle = (\overline{h^*})^{\mathrm{T}} \bullet h = 1.$$

A direct calculation yields that

$$h_1 = \frac{\mathrm{i}\omega + d_1 n_0^2 - a_{11}}{a_{12}}, \quad h_1^* = \frac{d_2 n_0^2 - \mathrm{i}\omega - a_{22}}{a_{12}} \quad \text{and}$$
$$l = \frac{a_{12}}{(d_1 + d_2)n_0^2 - 2\mathrm{i}\omega - a_{11} - a_{22}}. \tag{22}$$

The solution of (21) is assumed to take the form,

$$U(x,t) = U\left(x, T_0, T_1, T_2, \ldots\right) = \sum_{k=1}^{+\infty} \varepsilon^k U_k\left(x, T_0, T_1, T_2, \ldots\right), \tag{23}$$

where

$$\begin{aligned} U\left(x,T_0,T_1,T_2,\ldots\right) &= (u,v)^T = \left(u\left(x,T_0,T_1,T_2,\ldots\right),\right.\\ &\quad \left. v\left(x,T_0,T_1,T_2,\ldots\right)\right)^{\mathrm{T}},\\ U_k\left(x,T_0,T_1,T_2,\ldots\right) &= (u_k,v_k)^T = \left(u_k\left(x,T_0,T_1,T_2,\ldots\right),\right.\\ &\quad \left. v_k\left(x,T_0,T_1,T_2,\ldots\right)\right)^{\mathrm{T}}. \end{aligned}$$

The derivative with respect to t is now transformed into

$$\frac{\partial}{\partial t} = \frac{\partial}{\partial T_0} + \varepsilon\frac{\partial}{\partial T_1} + \varepsilon^2\frac{\partial}{\partial T_2} + \cdots = D_0 + \varepsilon D_1 + \varepsilon^2 D_2 + \cdots, \tag{24}$$

with the differential operator $D_i = \frac{\partial}{\partial T_i},\ i \in \mathbb{N}_0$.

To deal with the delayed terms, we expand $u(x,t-1)$ at $u(x,T_0-1,T_1,T_2,\ldots)$, and then have

$$u(x,t-1) = \varepsilon u_{11} + \varepsilon^2 u_{21} + \varepsilon^3 u_{31} - \varepsilon^2 D_1 u_{11} - \varepsilon^3 D_1 u_{21} - \varepsilon^3 D_2 u_{11} + \cdots, \tag{25}$$

where $u_{j1} = u_j\left(x,T_0-1,T_1,T_2,\ldots\right),\ j \in \mathbb{N}_0$.

Substituting (23)–(25) into (21), we obtain a set of ODEs associated with different powers of ε. First, for the ε-order terms, we have

$$\begin{cases} D_0 u_1 - \tau_c\left(d_1\Delta u_1 + a_{11}u_1 + a_{12}v_1 - \dfrac{ru_*\hat{u}_1}{N}\right) = 0,\\ D_0 v_1 - \tau_c\left(d_2\Delta v_1 - \eta v_*\Delta u_{1,1} + a_{21}u_1 + a_{22}v_1\right) = 0, \end{cases} \tag{26}$$

where a_{11}, a_{12}, a_{21} and a_{22} are given in (8). Thus, the solution of (26) can be expressed in the form of

$$\begin{cases} u_1 = G\left(T_1,T_2,\ldots\right)\mathrm{e}^{\mathrm{i}\omega\tau_c T_0}\cos(n_0x) + \text{c.c.},\\ v_1 = G\left(T_1,T_2,\ldots\right)\mathrm{e}^{\mathrm{i}\omega\tau_c T_0}h_1\cos(n_0x) + \text{c.c.}, \end{cases} \tag{27}$$

where h_1 is given in (22), and c.c. represents the complex conjugate of the previous term. Next, for the ε^2-order terms, we obtain

$$\begin{cases} D_0u_2 - \tau_c\left(d_1\Delta u_2 + a_{11}u_2 + a_{12}v_2 - \dfrac{ru_*\hat{u}_2}{N}\right)\\ = -D_1u_1 + \mu\left(d_1\Delta u_1 + a_{11}u_1 + a_{12}v_1 - \dfrac{ru_*\hat{u}_1}{N}\right)\\ \quad - \tau_c m\,u_1\left[\dfrac{v_1}{(u^*+1)^2} - \dfrac{v^*u_1}{(u^*+1)^3} + \dfrac{r\hat{u}_1}{mN}\right],\\ D_0v_2 - \tau_c\left(d_2\Delta v_2 - \eta v_*\Delta u_{2,1} + a_{21}u_2 + a_{22}v_2\right)\\ = -D_1v_1 + \tau_c\eta\left[v^*D_1\Delta u_{1,1} - (v_1)_x(u_{1,1})_x - v_1\Delta u_{1,1}\right]\\ \quad + \mu\left(d_2\Delta v_1 + a_{22}v_1 + a_{21}u_1\right)\\ \quad + \tau_c mc\,u_1\left[\dfrac{v_1}{(u^*+1)^2} - \dfrac{v^*u_1}{(u^*+1)^3}\right]. \end{cases} \tag{28}$$

Substituting the solution (27) into the right side of Eq. (28), and denoting the coefficient vector of $\mathrm{e}^{\mathrm{i}\omega\tau_c T_0}$ as m_1, which satisfies the solvability condition,

$$\langle h^*, (m_1, \cos(n_0x))\rangle = 0,$$

we obtain

$$\frac{\partial G}{\partial T_1} = M_1\mu G, \tag{29}$$

where

$$M_1 = \frac{\overline{h_1^*}(a_{11}+a_{12}-n_0^2d_1) - d_2h_1n_0^2 + a_{22}h_1 + a_{21}}{\overline{h_1^*} + h_1 + n_0^2\tau_c\eta v^*\mathrm{e}^{-\mathrm{i}\omega\tau_c}}.$$

Now, suppose that the solution to Eq. (28) is given in the form of

$$\begin{cases} u_2 = \displaystyle\sum_{k=0}^{+\infty}\left(\eta_{0,k}G\bar{G} + \eta_{1,k}\mathrm{e}^{2\mathrm{i}\omega\tau_c T_0}G^2 + \bar{\eta}_{1,k}\mathrm{e}^{-2\mathrm{i}\omega\tau_c T_0}\bar{G}^2\right)\cos(kx),\\ v_2 = \displaystyle\sum_{k=0}^{+\infty}\left(\zeta_{0,k}G\bar{G} + \zeta_{1,k}\mathrm{e}^{2\mathrm{i}\omega\tau_c T_0}G^2 + \bar{\zeta}_{1,k}\mathrm{e}^{-2\mathrm{i}\omega\tau_c T_0}\bar{G}^2\right)\cos(kx). \end{cases} \tag{30}$$

Let $c_k = \langle\cos(n_0x)\cos(n_0x),\cos(kx)\rangle = \int_0^\pi \cos(n_0x)\cos(n_0x)\cos(kx)\mathrm{d}x$. Then, we have

$$c_k = \int_0^\pi \cos^2(n_0x)\cos(kx)\mathrm{d}x = \begin{cases} \frac{\pi}{4}, & k = 2n_0 \neq 0,\\ \frac{\pi}{2}, & k = 0,\ n_0 \neq 0,\\ \pi, & k = n_0 = 0,\\ 0, & \text{otherwise}. \end{cases}$$

To obtain the solutions for $\eta_{0,k}$, $\eta_{1,k}$, $\zeta_{0,k}$ and $\zeta_{1,k}$, we substitute the solutions given in (27) and (30) into (28), then make the inner product with $\cos(kx)$ on both sides of the obtained equation, where $k \in \mathbb{N}_0$, and finally combine the obtained results to compare the coefficients of the terms G^2 and $G\bar{G}$.

For the ε^3-order terms, we omit the terms involving μ to get

$$\begin{cases} D_0u_3 - \tau_c\left(d_1\Delta u_3 + a_{11}u_3 + a_{12}v_3 - \dfrac{ru_*\hat{u}_3}{N}\right),\\ = -D_1u_2 - D_2u_1 - \tau_c m\left[\dfrac{u_1v_2+u_2v_1}{(u^*+1)^2} - \dfrac{u_1(2v^*u_2+u_1v_1)}{(u^*+1)^3} + \dfrac{v^*u_1^3}{(u^*+1)^4}\right]\\ \quad - \dfrac{\tau_c r}{N}\left(u_2\hat{u}_1 + u_1\hat{u}_2\right) + O(\mu),\\ D_0v_3 - \tau_c\left(d_2\Delta v_3 - \eta v_*\Delta u_{3,1} + a_{21}u_3 + a_{22}v_3\right)\\ = -D_1v_2 - D_2v_1 + \tau_c\eta\left[(v_1)_x(D_1u_{1,1})_x - (v_2)_x(u_{1,1})_x - (v_1)_x(u_{2,1})_x\right.\\ \quad \left. - v_2\Delta u_{1,1}\right]\\ \quad + \tau_c\eta\left(v_1D_1\Delta u_{1,1} + v^*D_1\Delta u_{2,1} - v_1\Delta u_{2,1} + v^*\Delta D_2u_{1,1}\right)\\ \quad + \tau_c mc\left[\dfrac{u_1v_2+u_2v_1}{(u^*+1)^2} - \dfrac{u_1(2v^*u_2-u_1v_1)}{(u^*+1)^3} + \dfrac{v^*u_1^3}{(u^*+1)^4}\right] + O(\mu). \end{cases} \tag{31}$$

Substituting the solutions given in (27) and (30) into the right side of (31), and denoting the coefficient vector of $\mathrm{e}^{\mathrm{i}\omega\tau_c T_0}$ as m_2, which satisfies the solvability condition,

$$\langle h^*, (m_2, \cos(n_0x))\rangle = 0,$$

we obtain (by neglecting the contributions from the terms involving μ)

$$\frac{\partial G}{\partial T_2} = M_2G^2\bar{G}, \quad \text{where} \quad M_2 = \frac{Q}{\overline{h_1^*} + h_1 + n_0^2\tau_c\eta v^*\mathrm{e}^{-\mathrm{i}\omega\tau_c}}, \tag{32}$$

in which

$$\begin{aligned} Q = &-\frac{\overline{h_1^*}\tau_c r}{N}(\eta_{0,0}+\eta_{1,0}) - \tau_c\eta n_0^2\left(\zeta_{0,2n_0}\mathrm{e}^{-\mathrm{i}\omega\tau_c} + \zeta_{1,2n_0}\mathrm{e}^{\mathrm{i}\omega\tau_c} + \eta_{0,2n_0}h_1\right.\\ &\left. + \eta_{1,2n_0}\overline{h_1}\right)\\ &+ 2\tau_c\eta n_0^2\left[C_{2n_0}\left(\zeta_{0,2n_0}\mathrm{e}^{-\mathrm{i}\omega\tau_c} + \zeta_{1,2n_0}\mathrm{e}^{\mathrm{i}\omega\tau_c}\right) + \zeta_{0,0}\mathrm{e}^{-\mathrm{i}\omega\tau_c} + \zeta_{1,0}\mathrm{e}^{\mathrm{i}\omega\tau_c}\right]\\ &+ 8\tau_c\eta n_0^2C_{2n_0}\left(h_1\eta_{0,2n_0} + \overline{h_1}\eta_{1,2n_0}\mathrm{e}^{-2\mathrm{i}\omega\tau_c}\right) + \frac{9\pi\tau_c v^*m}{2(u^*+1)^4}\left(c - \frac{\overline{h_1^*}}{4}\right)\\ &+ \frac{2\tau_c m}{(u^*+1)^2}\left\{C_0\left[v^*c(\eta_{0,0}h_1 + \eta_{1,0}\overline{h_1}) + c(\zeta_{0,0}+\zeta_{1,0})\right.\right.\\ &\left. - \overline{h_1^*}(\eta_{0,0}+\eta_{1,0}+\zeta_{0,0}+\zeta_{1,0})\right]\\ &\qquad + C_{2n_0}\left[v^*c(\eta_{0,2n_0}h_1 + \eta_{1,2n_0}\overline{h_1})\right.\\ &+ c(\zeta_{0,2n_0}+\zeta_{1,2n_0}) - \overline{h_1^*}(\zeta_{0,2n_0}+\zeta_{1,2n_0})\right]\\ &\qquad \left.\left. - \frac{\pi}{4}\overline{h_1^*}(\eta_{0,2n_0}+\eta_{1,2n_0})\right\}\right.\\ &+ \frac{\tau_c m}{8(u^*+1)^3}\left\{16v^*(h_1^*\pi - 2cC_0)(\eta_{0,0}+\eta_{1,0})\right.\\ &+ 8v^*(3h_1^* - 4cC_{2n_0})(\eta_{0,2n_0}+\eta_{1,2n_0})\\ &\qquad \left. + 3\pi\left[\overline{h_1^*}(2h_1+\overline{h_1}) - 4c(h_1+2\overline{h_1})\right]\right\}. \end{aligned}$$

Therefore, the normal form of the n_0-mode Hopf bifurcation for system (2) describing the dynamics on the centre manifold is given by

$$\dot{G} = M_1\mu G + M_2G^2\bar{G}, \tag{33}$$

where M_1 and M_2 are given by (29) and (32), respectively.

Let $G = re^{i\theta}$. Then, the normal form of Hopf bifurcation for system (2) given in polar coordinate up to 3rd-order terms can be written as

$$\begin{cases} \dot{r} = \mathrm{Re}(M_1)\mu r + \mathrm{Re}(M_2)r^3, \\ \dot{\theta} = \mathrm{Im}(M_1)\mu + \mathrm{Im}(M_2)r^2. \end{cases} \tag{34}$$

Therefore, based on the normal form (34) and by a standard analysis, for example, see [28], we have the following theorem for the n_0-mode Hopf bifurcations for the system (2).

Theorem 4.1. *For the normal form (34), when* $\frac{\mathrm{Re}(M_1)\mu}{\mathrm{Re}(M_2)} < 0$, *the first equation in (34) has a nontrivial equilibrium* $r^* = \sqrt{-\frac{\mathrm{Re}(M_1)\mu}{\mathrm{Re}(M_2)}}$, *implying that there exists periodic solutions near the PCSS* $E_* = (u^*, v^*)$ *of the system (2). Moreover, the following results hold.*

(1) If $\mathrm{Re}(M_1)\mu < 0$, *then the bifurcating periodic solutions are unstable, and the direction of bifurcation is forward (backward) when* $\mu > 0$ ($\mu < 0$).

(2) If $\mathrm{Re}(M_1)\mu > 0$, *the bifurcating periodic solutions are stable, and the direction of bifurcation is forward (backward) when* $\mu > 0$ ($\mu < 0$).

5. Numerical simulation

In this section, we use the real data taken from the forest industry and the experimental data in [29–33], to numerically investigate the spatio-temporal dynamics, and compare the simulations with the theoretical results obtained in the previous sections.

5.1. Parameter estimation

In order to simulate our new model (2) with realistic parameter values, we select the real data from a typical pine wood nematode epidemic area in Yuan'an County, Hubei Province, China, located in the middle and upper reaches of the Yangtze River in Northwest Hubei Province, for which there is a temperate climate having four distinct seasons and abundant rainfall. The area of forest is about 13.87×10^4 hm^2, where the unit hm^2 denotes *hectares*, which is included in the National Natural Forest Protection Project (NNFPP), with the forest coverage rate around 76%. The pine forest community is one of the climax communities in this region, and the area also has the most widely distributed natural forest type. Pinus massoniana, as a typical forest type in subtropical zone, occupies 26.5% in this region [29]. This area was declared a pine wilt disease epidemic area in 2019 (released by the China National Forestry and Grassland Administration). The pine wood nematode epidemic killed 12×10^4 pine trees, caused huge economic losses, where the disease was mainly transmitted by the vector insect, M. alternatus, carrying the pine wood nematode.

In the following, we estimate the values or ranges for some key system parameters based on the data posted by the National Forestry and Grassland Administration of China (http://www.forestry.gov.cn/) and the experimental data used in [29–33].

(1) Estimation of the natural growth rate of M. alternatus r: Based on the studies on the energy required for maintaining life activities such as reproduction by using fresh Masson pine as supplementary nutrition after the emergence of monochamus alternatus, the daily average egg production of female adults of M. alternatus is given in Table 1.

The birth rate of M. alternatus is defined as

$$\text{Birth rate} = \frac{\text{egg production per month}}{\text{egg production per month} + \text{initial quantity}}.$$

Thus, we select the average of feeding on the mixed branches, current-year-grown branches, 2-years-grown branches and 3-years-grown branches, as the average daily fecundity of female adult M. alternatus, namely,

$$\text{Average daily amount of eggs} = \frac{2.03 + 3.21 + 1.26 + 1.18}{4} = 1.92/\text{per day}.$$

Table 1
Average daily fecundity of female adult M. alternatus [29].

Project	Mixed branches	current-year branches	2-years branches	3-years branches
Number of egg cages	6	8	4	2
Average daily amount of eggs	2.03	3.21	1.26	1.18

Table 2
Field trapping results of the case area [30].

Year	Monitoring area	Amount	Male	Female	Male–female ratio
2019	A: 243.8 hm^2	1973	1241	732	1.695
2020	B: 148.5 hm^2	1938	1181	757	1.56
Sum		3911	2422	1489	1.6275

Hence, the average monthly amount of eggs is equal to $\frac{1.92\times 365}{12} = 58.4$.

We know that M. alternatus has significant differences in the ratio of male to female in different climatic conditions and geographical latitudes. Based on the surveillance data of the selected case area (see Table 2), it has been found that the male–female ratio was 1.696 and 1.56, respectively, and thus we take the average value $\frac{1.695+1.56}{2} = 1.6275$.

Suppose that the initial number of the female M. alternatus in the population of the case area is u_0, which can be calculated according to the birth rate definition as $\frac{58.4u_0}{58.4u_0+(1+1.6275)u_0} \approx 0.9569$.

It was shown in [31] that the natural mortality of M. alternatus is 0.011764. In conclusion, the natural rate of growth of M. alternatus is equal to

$$\text{Birth rate} - \text{mortality} = 0.9569 - 0.011764 \approx 0.95.$$

Thus, we select $r = 0.95$.

(2) Estimation of the capacity of environmental for M. alternatus N: Note that the forest area of Yuan'an county is 13.87×10^4 hm^2, and the pinus massoniana forest occupies 26.5%, and so the area is about $13.87 \times 26.5\% \approx 3.68 \times 10^4$ hm^2 in this region. Note here that the unit 10^4 hm^2 is often used in China for measuring land areas, called "Wan Gongqing" which equals $\frac{1}{100}$ million hectares. According to the monitoring area and amount in Table 2, the amount of M. alternatus in the whole region is about (29.78×10^4~47.97×10^4). By noticing that the environmental capacity is higher than the actual number of M. alternatus, yet not exceeding too much of the actual number since there exist many M. alternatus when the PWD occurs, we select the value of N as 2–4 times of the actual number of M. alternatus. Thus, we choose $N = 100$ ($\times 10^4$ hm^2) for the capacity of environmental of M. alternatus, that is $N = 100$.

(3) Estimation of the mortality of M. alternatus induced by chemical control and physical control b_1, and the mortality of M. alternatus induced by parasitical enemy and pathogenic microorganism k: According to the data from the official website of the National Forestry and Grassland Administration (http://www.forestry.gov.cn/, accessed on Oct. 10, 2023), we obtain the control rate of forest diseases in China for the years from 2005 to 2021, which are plotted in Fig. 3.

It is seen from Fig. 3 that the control rate is about 60% ~ 80%, but actually, as we all know, the control measures efficiency is mainly maintained at 20%~50%. Thus, we select the mortality of M. alternatus induced by chemical control and physical control, $b_1 = 0.25 \in (60\% \times 20\%, 80\% \times 50\%) = (12\%, 40\%)$, where the value of b_1 has been chosen close to the median since we are more interested in the biological control. Moreover, we may as well assume that the mortality of M. alternatus induced by parasitical enemy and pathogenic microorganism (k) is much less than the mortality of M. alternatus induced by chemical control and physical control (b_1), and thus we take $k = \frac{b_1}{25} = 0.01$.

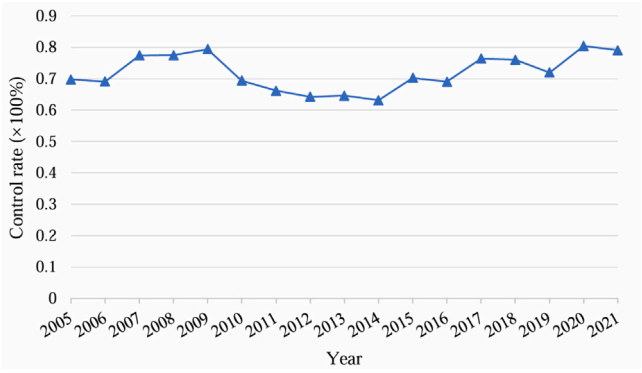

Fig. 3. Forest disease control rate in China for the years 2005–2021.

(4) Estimation of the encounter rate of the M. alternatus and woodpecker m and the conversion rate of the generalist woodpecker c: The pecking rate (a direct reflection of predation intensity) of woodpecker to M. alternatus is defined as the percentage of the total population of a particular M. alternatus that is preyed by woodpecker upon within a certain range, that is,

$$\text{Pecking rate} = \frac{\text{the number of insects pecked}}{\text{the total number of insects}} \times 100\%.$$

In fact, the encounter rate of the M. alternatus and woodpecker m can be described by using the pecking rate of woodpecker to M. alternatus. The experiment in Wulate Front County of Bayannaoer League of China [32] showed that the average pecking rate of the spotted woodpecker (a type of woodpecker) on anoplophora glabripennis (a type of longicorns beetle) is about 72.3%. Considering that the pecking rate of different woodpeckers may vary slightly in different regions, we select an approximation for the encounter rate of the M. alternatus and woodpecker as $m = 0.7$.

It is well known that the conversion rate of the functional response depends on different species. Many published results chose the conversion rate of predator–prey model in $(0, 1)$ [34–36]. Thus, it is reasonable to choose the conversion rate of the generalist woodpecker $c = 0.6 \in (0, 1)$ for the study of our model (2).

(5) Estimation of the mortality of woodpecker b_2: It has been shown in [33] that the main causes of death of woodpecker are predation and natural death, and the average survival and mortality rates are 57.4% and 42.6%, respectively. Taking into account the difference from regions and the effect of chemical control, environmental and other factors on woodpecker mortality, we choose $b_2 = 0.5$ which is a little bit larger than 42.6%.

In addition, it is known that the diffusion coefficient for woodpecker is higher than that of M. alternatus, that is, $d_2 > d_1$. Woodpeckers have memories, but their ability to spread of memory-based diffusion is much lower than higher animals, and so we select $\eta = 0.02$.

Summarizing the above discussions, we have the following estimation for the parameters to be used in our simulation of the model (2):

$$\begin{aligned} &d_1 = 0.01,\ d_2 = 0.02,\ r = 0.95,\ N = 100,\ m = 0.7,\\ &c = 0.6,\quad \eta = 0.02,\ k = 0.01,\ b_1 = 0.25,\ b_2 = 0.5. \end{aligned} \tag{35}$$

5.2. Simulation of model (2)

The simulation is focused on the PWD biological control by releasing woodpecker, and pay particular attention to the effect of the input rate Λ on the existence and stability of the PCSS of the system (2). Fig. 4 shows the case $b_2 - cm > 0$ in Lemma 3.1(3) (the cases $b_2 - cm \le 0$ are simple) for the existence and stability of the PCSS in system (2), for which the parameter values are given in (35). Fig. 4(a) depicts the expressions A_0 and F_0 under the assumption (H_1) with respect to the input rate Λ, that is, $A_0(u_k^*) = \frac{ru_k^*}{N} - a_{11} - a_{22}$ and $F_0(u_k^*) = a_{11}a_{22} - a_{12}a_{21} - \frac{ru+k^*a_{22}}{N}$, $k = 1, 2$. It is seen from Fig. 4(a) that the system (2) has a unique LAS PCSS E_1 when $\Lambda \in [0, 0.493)$ due to that the condition (H_1): $A_0(u_1^*) > 0$ and $F_0^*(u_1^*) > 0$, always holds. When $\Lambda \in (0.493, 1.688)$, the system (2) has two PCSS E_1 and E_2, which coincide at $\Lambda = 1.688$. Obviously, E_1 is LAS due to that the condition (H_1) always holds, and E_2 is always unstable because of $F_0(u_2^*) < 0$.

In order to better explain the results in Fig. 4(a), we particularly show the values of the PCSS $u_{1,2}^*$ and $v_{1,2}^*$ of the system (2) with respect to the input rate Λ, see Fig. 4(b). It can be observed from Fig. 4 that the system (2) does not have PCSS for $\Lambda > 1.688$. Actually, large input rate Λ leads to a sharp decline of the amount of M. alternatus, which may affect the survival of woodpecker and destroy the balance of natural ecological environment. When Λ is small ($\Lambda \in [0, 0.493)$), $u_1^* \gg v_1^*$, implying that the amount of M. alternatus is much larger than that of woodpeckers, which is consistent with the fact that a woodpecker can peck a large number of M. alternatus, and thus ecosystem is in a steady state and the PCSS (u_1^*, v_1^*) is LAS. With an increase of Λ, the value of u_1^* decreases while v_1^* increases, yielding $u_1^* \gg v_1^*$, and so the PCSS (u_1^*, v_1^*) is also LAS. While when $\Lambda \in (0.493, 1.688)$, another steady state (u_2^*, v_2^*) occurs. Note that u_2^* is about the same size as that of v_2^* even in the early development of Λ in this region, $u_2^* < v_2^*$, which contradicts with the fact that the number of M. alternatus should be much larger than the number of woodpeckers. Thus, (u_2^*, v_2^*) is unstable. The above theoretical analysis results are consistent with the actual ecosystem. In fact, a single woodpecker can peck a lot of M. alternatus when the ecosystem is in a steady state, while if the value of u_2^* is close to or smaller than $v_2 *$, the PCSS (u_2^*, v_2^*) cannot be stable.

To investigate the cost of biological control, we choose a small input rate $\Lambda = 0.2$, with other parameter values given in (35). Then, it follows from (5) that

$$a_0 = m\Lambda + b_2(b_1 + k - r) = -0.2050 < 0,$$

which, by Lemma 3.1, shows that the system (2) has a unique PCSS,

$$E_* = (u^*, v^*) = \left(\frac{-a_1 + \sqrt{a_1^2 - 4a_0a_2}}{2a_2},\ \frac{\Lambda(u_1^* + 1)}{b_2(u_1^* + 1) - cmu_1^*}\right) \approx (70.2227,\ 2.3284).$$

Next, we derive the stability conditions for the constant steady state E_* and possible bifurcating periodic solutions for system (2) with and without nonlocal effect and memory diffusion, respectively.

(1) Without diffusion: Obviously (H_1) and (H_2) hold. By Theorem 3.2, the positive equilibrium E_* of the system (2) without diffusion is LAS.

(2) Without nonlocal effect and memory diffusion: A direct calculation using (13) with $p_1 = p_2 = p_3 = 0$ shows that

$$\delta = \left[d_2\left(\frac{ru^*}{N} - a_{11}\right) - d_1a_{22}\right]^2 - 4d_1d_2F_0 = 1.4466 \times 10^{-4},$$
$$d_2\left(a_{11} - \frac{ru^*}{N}\right) + d_1a_{22} = -0.0138, \quad l(1) = 0.0694,$$

which satisfies the condition (2) in Theorem 3.3, implying that E_* is LAS.

(3) With nonlocal effect but without memory diffusion: Through the calculation using (13) with $p_1 = p_2 = 1$, $p_3 = 0$, we obtain

$$\delta = (d_2a_{11} + d_1a_{22})^2 - 4d_1d_2(a_{11}a_{22} - a_{12}a_{21}) = 1.6102 \times 10^{-6},$$
$$d_2a_{11} + d_1a_{22} = -4.0772 \times 10^{-4},$$
$$l(1) = -0.0012,$$

which does not satisfy any of conditions in Theorem 3.3, and thus E_* is unstable, indicating that the nonlocal effect induces a stability switch of the PCSS E_*.

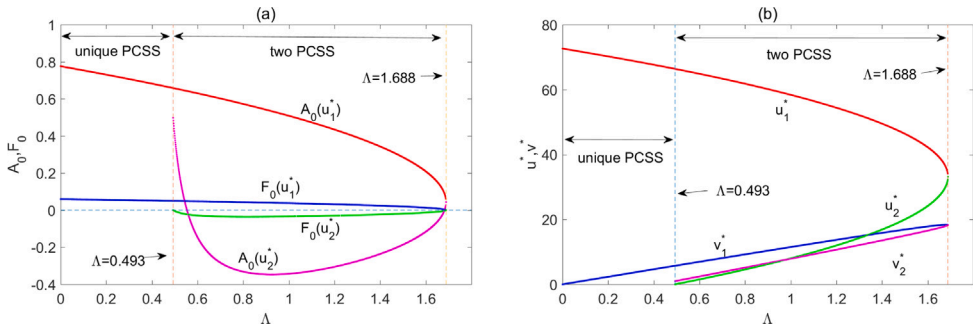

Fig. 4. Existence and stability of the PCSS of system (2) with respect to the input rate Λ: (a) the functions A_0 and F_0; and (b) the values of PCSS u^* and v^*.

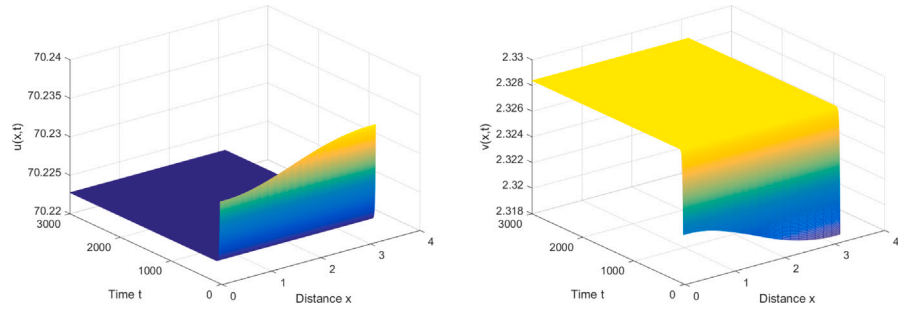

Fig. 5. The LAS PCSS E_* of the system (12) for $\tau = 3$.

(4) With memory diffusion but without nonlocal effect: Note that from (13) with $p_1 = p_2 = 0,\ p_3 = 1$, we have

$$\delta = 0.0021 \geq 0, \quad d_2(a_{11} - \frac{ru^*}{N}) + d_1 a_{22} + a_{12}\eta v^* = -0.0459, \quad l(1) = 0.1016,$$

showing that the parameters satisfy the condition (2) in Theorem 3.3, and thus E_* is LAS when $\tau = 0$. Now Eq. (14) with $p_1 = p_2 = 0,\ p_3 = 1$ becomes

$$h(z) = z^2 + (A_n^2 - 2F_n)z + F_n^2 - C_n^2 = 0, \quad n \in \mathrm{N}_+, \quad z = \omega^2.$$

A careful examination shows that $F_n \geq 0$ for all n when $d_2(\frac{ru^*}{N} - a_{11}) - d_1 a_{22} > 0$ and (H_1) holds, yielding $F_n + C_n \geq 0$ due to $C_n = -a_{12}n^2\eta v^* > 0$. Therefore, we only need to determine the sign of $F_n - C_n = (d_1 n^2 + \frac{ru^*}{N} - a_{11})(d_2 n^2 - a_{22}) - a_{12}a_{21} + a_{12}n^2\eta v^*$. By a simple calculation, we obtain that

$$\begin{aligned} &F_2 - C_2 = -0.0149, \quad F_3 - C_3 = -0.0938, \quad F_4 - C_4 = -0.1875,\\ &F_5 - C_5 = -0.2792, \quad F_6 - C_6 = -0.3473, \quad F_7 - C_7 = -0.3654,\\ &F_8 - C_8 = -0.3022, \quad F_9 - C_9 = -0.1218, \quad F_n - C_n > 0, \forall\ n \geq 10. \end{aligned}$$

Moreover, it is easy to prove that $A_n^2 - 2F_n > 0$ for all n as follows. Denoting $y = n^2$, we obtain $L(y) = A_n^2 - 2F_n = (d_1^2 + d_2^2)y^2 + 2(\frac{d_1 ru^*}{N} - d_1 a_{11} + d_2 a_{22})y + A_0^2 - 2F_0$. It is easy to see that the graph of the quadratic function $L(y)$ opens upward, and its vertex is located on the negative y-axis with $L(0) > 0$ by using the parameter values given in (35). This implies that $L(y) > 0$ for all $y > 0$. Further, by a simple computation using (15), we obtain that

$$\begin{aligned} &\tau_{2,1}^{(0)} = 30.1158, \quad \tau_{3,1}^{(0)} = 7.8354, \quad \tau_{4,1}^{(0)} = 4.7136, \quad \tau_{5,1}^{(0)} = 3.7035,\\ &\tau_{6,1}^{(0)} = 3.4005, \quad \tau_{7,1}^{(0)} = 3.5374, \quad \tau_{8,1}^{(0)} = 4.2872, \quad \tau_{9,1}^{(0)} = 7.8008. \end{aligned}$$

According to Theorem 3.4(2)(a), $I_1 = \{n_{k1}, n_{k2}, \dots, n_{km}\} = \{2,3,4,5,6,7,8,9\}$, $\tau^* = \tau_{6,1}^{(0)} = 3.4005$, so the PCSS $E_* = (u^*, v^*)$ of the system (12) is LAS for $0 < \tau < \tau^*$ and unstable for $\tau > \tau^*$. Moreover, the system (12) undergoes Hopf bifurcation at $\tau = \tau_{n_k,1}^{(j)}$ $(n_k = 2,3,4,\dots,9)$. The detailed computation of the normal form for the Hopf bifurcation of the system (12) is similar to that for the system (2), and is thus omitted here for brevity. A simple computation shows that the bifurcating periodic solutions are unstable for $\tau = \tau^*$ near the PCSS. The PCSS is LAS for $\tau = 3 < \tau^* = \tau_{6,1}^{(0)} = 3.4005$, as shown in Fig. 5.

(5) With nonlocal effect and memory diffusion with $p_1 = p_2 = p_3 = 1$ in (13): By a straightforward calculation, we obtain

$$\delta \geq 0, \quad d_2 a_{11} + d_1 a_{22} + a_{12}\eta v^* < 0 \quad \text{and} \quad l(1) > 0,$$

which indicates that the condition (2) in Theorem 3.3 is satisfied, and so E_* is LAS for $\tau = 0$. Now Eq. (14) with $p_1 = p_2 = p_3 = 1$ becomes

$$\begin{aligned} h(z) =& z^2 + \left[\left(A_n - \frac{ru^*}{N}\right)^2 - 2F_n - 2\left(a_{22} - d_2 n^2\right)\frac{ru^*}{N}\right]z\\ &+ \left[F_n + \left(a_{22} - d_2 n^2\right)\frac{ru^*}{N}\right]^2 - C_n^2 = 0, \quad n \in \mathrm{N}_+, \quad z = \omega^2. \end{aligned}$$

It is easy to prove that $F_n + (a_{22} - d_2 n^2)\frac{ru^*}{N} + C_n > 0$ for all integers $n \geq 1$, and $F_n + (a_{22} - d_2 n^2)\frac{ru^*}{N} - C_n$, as shown in Fig. 6, is negative for $n = 1, 2, \dots, 12$, and positive for the integers $n \geq 13$.

Moreover, it is also easy to prove that $P_n = \left(A_n - \frac{ru^*}{N}\right)^2 - 2F_n - 2\left(a_{22} - d_2 n^2\right)\frac{ru^*}{N} > 0$ since the value of the quadratic function at its vertex is negative, while the intersection point with the n-axis is located on the positive axis. Fig. 7 depicts the critical curves: τ_n^0, $n = 1, 2, \dots, 12$. Thus, according to Theorem 3.4(2)(a), $I_1 = \{n_{k1}, n_{k2}, \dots, n_{km}\} = \{1, 2, \dots, 12\}$, $\tau^* = \tau_4^{(0)} = \min\{\tau_n^{(0)} | n = 1, 2, \dots, 12\} = 1.1665$. Then, the PCSS $E_* = (u^*, v^*)$ of the system (2) is LAS for $0 < \tau < \tau^*$ and unstable for $\tau > \tau^*$. Moreover, the system (2) undergoes Hopf bifurcation at $\tau = \tau_{n,1}^{(j)}, n = 1, 2, \dots, 12$. The positive equilibrium is LAS for $\tau = 1 < \tau^* = \tau_4^{(0)} = 1.1665$, see Fig. 8.

When $\tau = 1.17 > \tau^* = \tau_4^{(0)} = 1.1665$, the stability of the PCSS will change through the first Hopf bifurcation critical point $\tau_4^{(0)}$. When $n = 4$, we obtain $z_1 = 0.4277$ and $\omega_1 = 0.6540$. It follows from the normal form of Hopf bifurcation (34) that $\mathrm{Re}(M_1) > 0$ and $\mathrm{Re}(M_2) < 0$, implying that the first equation in (34) has one nontrivial equilibrium when $\mu > 0$, and thus the inhomogeneous periodic solutions of system (2) for the 4-mode Hopf bifurcation

Table 3
Comparison of the dynamical behaviours for 5 cases of system (2).

Model	Stability of the constant steady state of E_* and periodic solutions arising from Hopf bifurcation
ODE	LAS, No Hopf bifurcation
ODE+self-diffusion	LAS, No Hopf bifurcation
ODE+self-diffusion+nonlocal	Unstable for $\tau \geq 0$, No Hopf bifurcation
ODE+self-diffusion +memory diffusion	LAS for $\tau \in [0, \tau_6^{(0)})$, unstable for $\tau > \tau_6^{(0)}$ unstable spatial inhomogeneous periodic solutions near the first Hopf bifurcation value $\tau_6^{(0)}$
ODE+self-diffusion+nonlocal +memory diffusion	LAS for $\tau \in [0, \tau_4^{(0)})$, unstable for $\tau > \tau_4^{(0)}$ stable spatial inhomogeneous periodic solutions near the first Hopf bifurcation value $\tau_4^{(0)}$

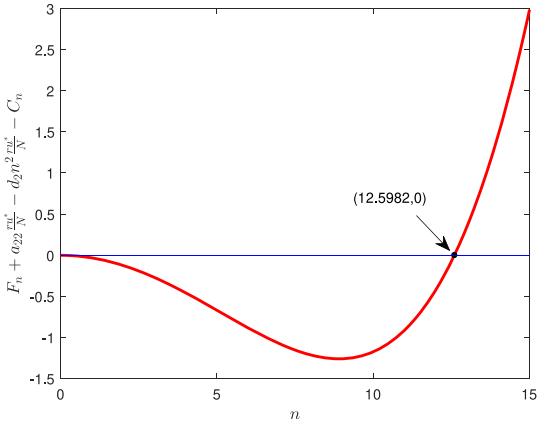

Fig. 6. The graph of $F_n + a_{22}\frac{ru^*}{N} - d_2 n^2 \frac{ru^*}{N} - C_n$ as a function in n.

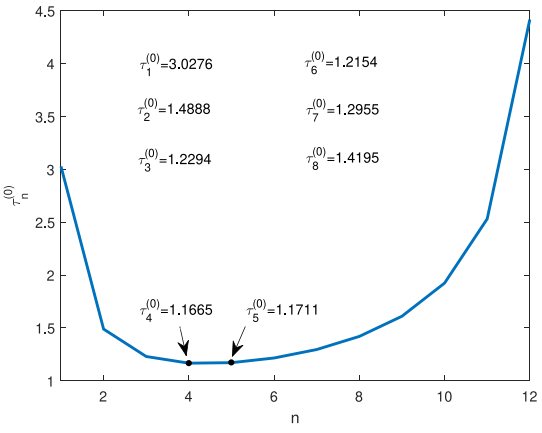

Fig. 7. Hopf bifurcation critical values $\tau_n^{(0)}$ for the system (2).

restricted on the centre manifold are stable. Fig. 9 shows that the solutions converge to the spatially inhomogeneous periodic solutions, which agree with the theoretical predictions.

Compared with the model having memory diffusion but without nonlocal effect, it is seen that the stable region for the constant steady state $E_* = (u^*, v^*)$ becomes smaller.

We summarize the above results in Table 3.

Unlike the results shown in the existing literature, for example, see [19,34], that the nonlocal competition can induce stable spatial inhomogeneous periodic solutions, however, in our model, there does not exist spatial periodic solutions, while the nonlocal competition can induce a stability switch on the stable PCSS E_*. Moreover, different from the results shown in [21,22,24] that the memory-based diffusion can induce stable spatial inhomogeneous periodic solutions, while our model undergoes Hopf bifurcation, yielding unstable spatial inhomogeneous periodic solutions. However, when both memory-based diffusion and nonlocal competition are involved in the model, the stability of the spatial inhomogeneous periodic solutions switches, that is, the model exhibits stable spatial inhomogeneous periodic solutions.

6. Conclusion and discussion

In this paper, we proposed an M. alternatus-woodpecker model with nonlocal competition and memory-based diffusion associated with the pine wilt disease control. First, we analysed the dynamical properties of the model with and without memory diffusion and nonlocal competition, and derived the conditions for the existence and stability of the constant steady state and the existence of Hopf bifurcation near the constant steady state. Then, we generalized the original multiple time scales method to derive the normal form of Hopf bifurcation for the reaction–diffusion equation with both memory-based diffusion and nonlocal competition, and considered the stability and direction of spatially inhomogeneous periodic solutions based on the obtained normal form. Finally, we estimated the system parameter values from real forest data and carried out numerical simulations.

Our results show that the nonlocal competition could cause the stable constant steady state to lose stability. Actually, when the competitive resources for M. alternatus are limited in one place, the M. alternatus will flee to other places to survive due to the nonlocal competition among the M. alternatus. As a result, the number of M. alternatus is hard to be kept stable. Moreover, the memory-based diffusion could induce unstable spatially inhomogeneous periodic solutions. When the memory diffusion ability of woodpecker is introduced to the model, woodpecker can increase the pecking rate during its memory period, thus effectively control the amount of M. alternatus, and achieve the goal of controlling the pine wilt disease. After the memory period, the pecking rate of woodpecker decreases so that the amount of M. alternatus can no longer be controlled stable. However, the combination of the memory diffusion and the nonlocal competition could induce the bifurcation of stable spatially inhomogeneous periodic solutions. This implies that the stability of spatial inhomogeneous periodic solutions may be different from the ones without nonlocal competition, explaining why the spatiotemporal heterogeneity problem exists in the forest diseases and pests, such as the breaking of spatiotemporal symmetry, the outbreak of spatial inhomogeneity, and the spatiotemporal periodic variability.

Our study reveals that the nonlocal competition of M. alternatus has greater influence on the stability of the constant steady state, and memory diffusion is easier to induce bifurcation of periodic solutions, showing that the memory-based diffusion is helpful to increase stability of the steady state solutions. Our study promotes further research related to the spatiotemporal heterogeneity problem in this area.

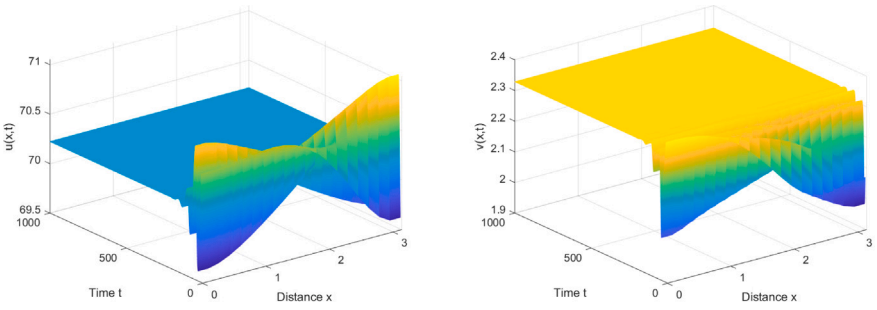

Fig. 8. The LAS PCSS E_* of the system (2) for $\tau = 1$.

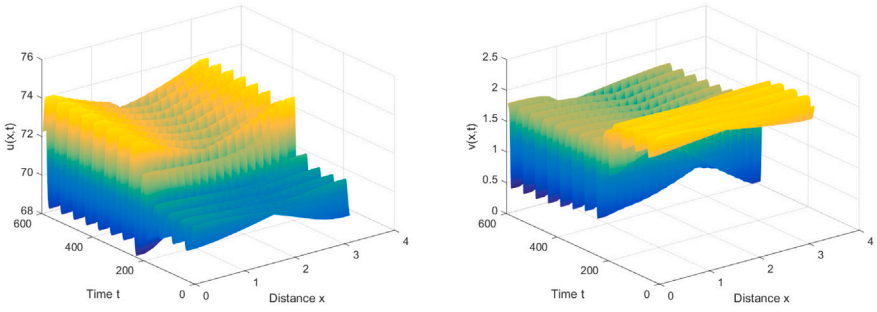

Fig. 9. Stable inhomogeneous periodic solutions of the system (2) near the PCSS E_* for $\tau = 1.17$.

CRediT authorship contribution statement

Yuting Ding: Writing – original draft, Validation, Methodology, Investigation, Formal analysis, Conceptualization. **Pei Yu:** Writing – review & editing, Validation, Supervision, Methodology, Investigation, Formal analysis.

Declaration of competing interest

The authors declare that they have no known competing financial interests or personal relationships that could have appeared to influence the work reported in this article.

Acknowledgements

The first author (Y. Ding) was supported by the National Natural Science Foundation of China, No. 12571525, and the second author (P. Yu) was supported by the Natural Sciences and Engineering Research Council of Canada, No. R2686A02.

Data availability

The data used in this manuscript are available from public sources.

References

[1] L. Chen, G. Msigwa, M. Yang, M. Yang, A.I. Osman, S. Fawzy, D.W. Rooney, P.-S. Yap, Strategies to achieve a carbon neutral society: a review, J. Env. Chem. Lett. 20 (2022) 2277–2310.
[2] J.P. Lee, S.S. Sekhon, J.H. Kim, S.C. Kim, B.-K. Cho, J.Y. Ahn, Y.H. Kim, The pine wood nematode bursaphelenchus xylophilus and molecular diagnostic methods, Mol. Cell. Toxicol. 17 (2021) 1–13.
[3] Z. Wang, C. Wang, Z. Fang, D. Zhang, L. Liu, M.R. Lee, Z. Li, J. Li, C. K.Sung, Advances in research of pathogenic mechanism of pine wilt disease, Afr. J. Microbiol. Res. 4 (2010) 437–442.
[4] F. Wang, Pine wilt in meteorological hazard environments, Nat. Hazards 72 (2014) 723–741.
[5] Q. Xu, X. Zhang, J. Li, J. Ren, Pine wilt disease in northeast and northwest China: a comprehensive risk review, Forests 14 (2023) 174.
[6] J. Ye, Epidemic status of pine wilt disease in China and its prevention and control techniques and counter measures, Sci. Silvae Sin. 55 (2019) 1–10.
[7] K. Lee, D. Kim, Global dynamics of a pine wilt disease transmission model with nonlinear incidence rates, Appl. Math. Model. 37 (2013) 4561–4569.
[8] A.U. Awan, M. Ozair, Q. Din, T. Hussain, Stability analysis of pine wilt disease model by periodic use of insecticides, J. Biol. Dyn. 10 (2016) 506–524.
[9] M. Khan, R. Khan, Y. Khan, S. Islam, A mathematical analysis of pine wilt disease with variable population size and optimal control strategies, Chaos Solitons Fractals 108 (2018) 205–217.
[10] K.S. Lee, A.A. Laschari, Stability analysis and optimal control of pine wilt disease with horizontal transmission in vector population, Appl. Math. Comput. 226 (2014) 793–804.
[11] G. Rahman, K. Shah, F. Haq, N. Ahmad, Host vector dynamics of pine wilt disease model with convex incidence rate, Chaos Solitons Fractals 113 (2018) 31–39.
[12] Q. Wang, M. Bi, S.J. Ma, L. Shi, B. Yang, Research on spatial pattern of monochamus alternatus's occurrence rate based on meteorological factors, For. Res. 28 (2015) 61–66.
[13] J. Furter, M. Grinfeld, Local vs nonlocal interactions in population dynamics, J. Math. Biol. 27 (1989) 65–80.
[14] A. Bayliss, V.A. Volpert, Complex predator invasion waves in a holling-tanner model with nonlocal prey interaction, Phys. D. 346 (2017) 37–58.
[15] M. Alfaro, I. Hirofumi, M. Masayasu, On a nonlocal system for vegetation in drylands, J. Math. Biol. 77 (2018) 1761–1793.
[16] S. Chen, J. Shi, Stability and Hopf bifurcation in a diffusive logistic population model with nonlocal delay effect, J. Differential Equations 253 (2012) 3440–3470.
[17] J. Fang, X. Zhao, Monotone wavefronts of the nonlocal Fisher–KPP equation, Nonlinearity 24 (2011) 3043–3054.
[18] S. Guo, Bifurcation in a reaction–diffusion model with nonlocal delay effect and nonlinear boundary condition, J. Differential Equations 289 (2021) 236–278.
[19] S. Wu, Y. Song, Q. Shi, Normal forms of double Hopf bifurcation for a reaction–diffusion system with delay and nonlocal spatial average and applications, Comput. Math. Appl. 119 (2022) 174–192.
[20] W. Fagan, M. Lewis, M. Auger-Methe, T. Avgar, S. Benhamou, G. Breed, L. LaDage, U.E. Schlel, W. Tang, Y.P. Papastamatiou, J. Forester, T. Mueller, Spatial memory and animal movement, Ecol. Lett. 16 (2014) 1316–1329.
[21] J. Shi, C. Wang, H. Wang, X.P. Yan, Diffusive spatial movement with memory, J. Dynam. Differential Equations 32 (2020) 979–1002.
[22] Y. Song, Y. Peng, T. Zhang, Double Hopf bifurcation analysis in the memory-based diffusion system, J. Dynam. Differential Equations 36 (2024) 1635–1676.
[23] Y. Wang, C. Wang, D. Fan, Dynamics of a diffusive competition model with memory effect and spatial heterogeneity, J. Math. Anal. Appl. 523 (2023) 126991.

[24] M. Liu, H. Wang, W. Jiang, Bifurcations and pattern formation in a predator–prey model with memory-based diffusion, J. Differential Equations 350 (2023) 1–40.
[25] Y. Song, S. Wu, H. Wang, Spatiotemporal dynamics in the single population model with memory-based diffusion and nonlocal effect, J. Differential Equations 267 (2019) 6316–6351.
[26] X. Zhang, H. Zhu, Q. An, Dynamics analysis of a diffusive predator–prey model with spatial memory and nonlocal fear effect, J. Math. Anal. Appl. 525 (2023) 127123.
[27] Y. Hou, Y. Ding, Dynamic analysis of pine wilt disease model with memory diffusion and nonlocal effect, Chaos, Solitons Fractals 179 (2024) 114480.
[28] S. Wiggins, Introduction To Applied Nonlinear Dynamical Systems and Chaos, Springer, NY, 1990.
[29] C. Lin, M. Lai, G. Lu, D. Cai, C. Zhou, J. Zhao, Impacts of adult feeding materials on female reproduction capacity of monochamus alternatus hope, For. Res. 4 (2003) 398–403.
[30] Z. Xiao, S. Jing, H. Liu, Population dynamics and spatial density distribution of monochamus alternatus based on GIS spatial statistics and trapping method-a case study of Yuan'an county in Hubei, For. Inven. Plan. 46 (2021) 54–60.
[31] E.S. Ahmed, S.Z. Rida, Y.A. Gaber, On the stability analysis and solutions of fractional order pine wilt disease model, Appl. Math. Inf. Sci. 14 (2020) 1137–1146.
[32] G. Li, X. Re, J. Zhang, Primary study on controlling a nop lop hora glabrip ennis motsch with woodpecker, For. Surv. Des. Inn. Mong. 23 (2000) 34–36.
[33] H. Wilkins, G. Ritchison, Drumming and tapping by red-bellied woodpeckers: description and possible causation, Field Ornithol 70 (1999) 578–586.
[34] Y. Liu, D. Duan, B. Niu, Spatiotemporal dynamics in a diffusive predator–prey model with group defense and nonlocal competition, Appl. Math. Lett. 103 (2020) 106175.
[35] W. Zuo, Y. Song, Stability and double-Hopf bifurcations of a gause-Kolmogorov-type predator–prey system with indirect prey-taxis, J. Dynam. Differential Equations 33 (4) (2021) 1917–1957.
[36] W. Chen, H. Yu, C. Dai, Q. Guo, H. Liu, M. Zhao, Stability and bifurcation in a predator–prey model with prey refuge, J. Biol. Syst. 31 (02) (2023) 417–435.